Yang et al. Cell Communication and Signaling (2024) 22:444
https://doi.org/10.1186/s12964-024-01826-0

Cell Communication and Signaling

RESEARCH Open Access

TRIM35 triggers cardiac remodeling by regulating SLC7A5-mediated amino acid transport and mTORC1 activation in fibroblasts

Boshen Yang[1†], Zhixiang Wang[1†], Kaifan Niu[1†], Taixi Li[1†], Tingting Tong[3], Suiji Li[2], Liuhang Su[2], Yan Wang[2], Chengxing Shen[1*], Xian Jin[1*], Juan Song[2*] and Xia Lu[1*]

Abstract

Background Cardiac maladaptive remodeling is one of the leading causes of heart failure with highly complicated pathogeneses. The E3 ligase tripartite motif containing 35 (TRIM35) has been identified as a crucial regulator governing cellular growth, immune responses, and metabolism. Nonetheless, the role of TRIM35 in fibroblasts in cardiac remodeling remains elusive.

Methods Heart tissues from human donors were used to verify tissue-specific expression of TRIM35. Fibroblast-specific Trim35 gene knockout mice ($Trim35^{cKO}$) were used to investigate the function of TRIM35 in fibroblasts. Cardiac function, morphology, and molecular changes in the heart tissues were analyzed after transverse aortic constriction (TAC) surgery. The mechanisms by which TRIM35 regulates fibroblast phenotypes were elucidated using liquid chromatography-tandem mass spectrometry (LC-MS/MS) and RNA sequencing (RNA-Seq). These findings were further validated through the use of adenoviral and adeno-associated viral transfection systems, as well as the mTORC1 inhibitor Rapamycin.

Results TRIM35 expression is primarily up-regulated in cardiac fibroblasts in both murine and human fibrotic hearts, and responds to TGF-β1 stimulation. Specific deletion of TRIM35 in cardiac fibroblasts significantly improves cardiac fibrosis and hypertrophy. Consistently, the overexpression of TRIM35 promotes fibroblast proliferation, migration, and differentiation. Through paracrine signaling, it induces hypertrophic growth of cardiomyocytes. Mechanistically,

†Boshen Yang, Zhixiang Wang, Kaifan Niu and Taixi Li contributed equally to this work.

*Correspondence:
Chengxing Shen
shencx@sjtu.edu.cn
Xian Jin
jinxianian@126.com
Juan Song
songjuan_ok@163.com
Xia Lu
xialu0292@163.com

Full list of author information is available at the end of the article

we found that TRIM35 interacts with, ubiquitinates, and up-regulates the amino acid transporter SLC7A5, which enhances amino acid transport and activates the mTORC1 signaling pathway. Furthermore, overexpression of SLC7A5 significantly reverses the reduced cardiac fibrosis and hypertrophy caused by conditional knockout of TRIM35.

Conclusion Our findings demonstrate a novel role of fibroblast-TRIM35 in cardiac remodeling and uncover the mechanism underlying SLC7A5-mediated amino acid transport and mTORC1 activation. These results provide a potential novel therapeutic target for treating cardiac remodeling.

Keywords Cardiac remodeling, Fibroblast activation, TRIM35, SLC7A5, Amino acid transport, mTORC1

Introduction

Cardiac remodeling refers to the structural and functional changes that occur in the heart in response to various physiological or pathological stimuli [1]. Prolonged exposure to pressure overload can lead to maladaptive remodeling, characterized by an increase in cardiomyocyte size, excessive myocardial fibrosis, remodeling of the extracellular matrix (ECM), and is often observed in conditions such as hypertension, aortic stenosis, or valvular diseases [2]. The mechanical stress imposed by pressure overload triggers a cascade of cellular and molecular events within the myocardium [3]. Cardiomyocytes, fibroblasts, endothelial cells, and immune cells interact dynamically to orchestrate the fibrotic response [4]. Researches on the role of cardiac fibroblasts in cardiac remodeling have revealed their pivotal significance in the pathological process [1]. Cardiac fibroblasts primarily contribute to the maintenance of myocardial structure and function through their roles in ECM synthesis, degradation, and remodeling [4]. Given their central role in fibrosis, targeting cardiac fibroblasts and understanding the mechanisms underlying pressure overload-induced cardiac remodeling are crucial for developing targeted therapeutic interventions.

The Tripartite Motif (TRIM) proteins are characterized by their tripartite motif domain consisting of RING, B-box, and coiled-coil domains, which confer various functional properties, including E3 ubiquitin ligase activity and protein-protein interaction capabilities [5]. The TRIM family has garnered considerable attention in the field of tissue remodeling due to its diverse roles in regulating cellular processes implicated in fibrotic pathology, particularly in fibroblasts [6–8]. Several TRIM proteins, such as TRIM8, TRIM16, TRIM25, TRIM32, and TRIM72, have been identified to regulate cardiac remodeling [9–13]. Recently, TRIM35, a protein that has not been extensively studied, has garnered the attention of researchers. It has been found to play a role in cancer, autoimmune diseases, and neurological disorders [14]. So far, limited research has shown that TRIM35 can play important roles in regulating cellular growth, immune responses, and neuronal protection [14–16], highlighting its significance for further investigation into its functions and mechanisms. However, the role of TRIM35 in fibroblasts during the progression of ventricular remodeling has not yet been studied.

Accumulating evidence has shown that TRIM35 controls critical turnover and stability processes of both nuclear and cytosolic proteins, like nuclear P53, LSD1, IRF5, and cytosolic PKM2, TRFA3, TIGAR [14, 17–20]. Although research has reported that TRIM35 can ubiquitinate and regulate the membrane proteins TLR7 and TLR9 [21], studies on the signaling mediated by TRIM35 in regulating membrane proteins remain relatively scarce. Amino acid transporters, as the membrane proteins, play a crucial role in regulating the activation of fibroblasts [22]. The large neutral amino acid transporter SLC7A5 has been demonstrated to transport amino acids, including leucine, glutamine, and arginine, which support cell growth by activating the protein kinase mammalian target of rapamycin complex 1 (mTORC1) [23, 24]. It has been reported that arginine is crucial for fibroblast proliferation and the synthesis of extracellular matrix components such as collagen [25]. Glutamine serves as an essential substrate for cellular metabolism, participating in fibroblast growth and metabolic activities [26]. Cysteine is involved in collagen cross-linking and fibroblast activation [27]. Therefore, the interplay between SLC7A5-mediated amino acid transport and cardiac fibroblast activation presents a promising avenue for investigating the pathogenesis of myocardial fibrosis and identifying novel therapeutic targets. Moreover, the expression of SLC7A5 was found to be regulated by the cytokine IL-1β through the NF-κB pathway in fibroblast-like synoviocytes [28]. The Slc7a5 is a novel gene responsive to hypoxia in a HIF-2α-dependent manner in differentiated neuronal cells [29]. Slc7a5 gene was identified as a target of miR-138-5p in retinoblastoma cells [30]. However, the mechanisms regulating the expression and functional levels of SLC7A5 in cardiac fibroblasts during the process of myocardial remodeling remain unclear.

In this study, we found that TRIM35 is primarily up-regulated in cardiac fibroblasts during pressure overload-induced ventricular remodeling. Fibroblast-conditional deficiency of TRIM35 significantly improves cardiac fibrosis, and cardiac hypertrophy. Furthermore, overexpression of TRIM35 promotes fibroblast proliferation,

migration, and differentiation. What's more, Trim35 knockout in fibroblasts mitigates hypertrophic growth of cardiomyocytes via paracrine signaling. Mechanistically, we discovered that TRIM35 ubiquitinates SLC7A5, and up-regulates its protein level, which enhances amino acid transport and activates the mTORC1 signaling pathway in cardiac fibroblasts. Our study provides the first evidence of the crucial role of TRIM35 in activating cardiac fibroblasts and orchestrating ventricular remodeling by regulating the amino acid transporter SLC7A5.

Materials and methods

Human tissue sampling

Human remodeling myocardium samples used in this study were obtained from excised interventricular septal tissues during surgical removal from hypertrophic cardiomyopathy (HCM) patients. Non-remodeling human heart samples were obtained from non-remodeling left atrial tissues, and all detailed information was included in Figure S1. Written informed consents were obtained from all patients included in this study. This study was approved by the Xiamen Cardiovascular Hospital (Permit Number: KY2024-020-01) and conformed to the ethical guidelines of the 1975 Declaration of Helsinki.

Experimental animals

Wild-type male C57BL/6J mice, 8 weeks old, and neonatal Sprague-Dawley rats were purchased from JieSiJie Laboratory Animal Co., Ltd (Shanghai, China). Conditional transgenic mice targeting Trim35 gene ($TRIM35^{f/f}$) were generated by Cyagen Co., Ltd (Suzhou, China) in the C57BL/6J background, were raised in the Xiamen University Laboratory Animal Center and kept under constant environmental conditions with 12-hour light/dark cycles and had ad libitum access to food and water. Exon 2–4 of the Trim35 gene were selected as conditional knockout region (cKO region). The knockout of Exon 2–4 resulted in loss of function of the mouse Trim35 gene. The Col1a2-Cre^{ERT} mice, containing a Cre-ERT recombinase gene were purchased from Cyagen Co., Ltd (Suzhou, China). Fibroblast-specific Trim35 gene knockout mice ($Trim35^{cKO}$) were created by crossing $Trim35^{f/f}$ mice with Col1a2-Cre^{ERT} mice. 6-week-old Col1a2-Cre^{ERT}-positive $TRIM35^{f/f}$ mice were intraperitoneally treated with 50 mg/kg of tamoxifen dissolved in corn oil for 5 consecutive days, followed by a one-week rest before undergoing either sham or TAC surgery. Investigations were conducted following the guidelines outlined in the Guide for the Care and Use of Laboratory Animals published by the US National Institutes of Health (NIH Publication No. 85−23, revised 1996). Every animal care and experimental protocol was approved by the Xiamen University Committee on Animal Care (Permit Number: XMULAC20220147).

Mice model of transverse aortic constriction (TAC) induced cardiac hypertrophy

The TAC surgical procedure was conducted following previously established protocols [31]. Male mice (8 weeks old, weighing 22–25 g) were anesthetized using a mixture of isoflurane (1.5%) and oxygen (0.5 L/min) and positioned on a temperature-controlled surgical table. The hearts were exposed via a left thoracotomy in the third intercostal space. The 27-Gauge needle was carefully placed alongside the transverse aorta and then ligated around the artery using a 5−0 suture, positioned between the first and second branches of the aortic arch. Subsequently, the wire was swiftly removed, resulting in constriction of the aortic arch to the diameter of the wire. For the sham control group, an identical surgical procedure was performed, excluding the ligation of the suture around the aorta. Sham-operated mice served as controls. Heart samples were collected at 4 weeks after surgery. The heart weight to body weight ratio (HW/BW) was calculated. Subsequently, heart samples were either flash-frozen in liquid nitrogen and stored at -80 °C for further RNA and protein analysis or fixed in a PBS solution containing 4% paraformaldehyde for histochemical analysis.

Echocardiography

Cardiac functions were evaluated using the Vevo 2100 High-Resolution Micro-Ultrasound System (FUJIFILM Visual Sonics Inc.). Mice were anesthetized with a mixture of isoflurane (1.5%) and oxygen (0.5 L/min) and positioned on a heated table in the supine position. Two-dimensional (2D) guided left ventricular M-mode tracings were obtained at the level of the papillary muscle in a short-axis view to quantify parameters such as ejection fraction (EF%) and fractional shortening (FS%). These measurements were performed by a researcher blinded to the experimental treatments to prevent biases and were averaged over five consecutive cardiac cycles.

Adenovirus (Adv)-mediated gene transfection into the myocardium in vivo

To establish a heart-overexpressed SLC7A5 animal model, we employed the cardiac adenoviral gene transfer approach. Adv-Flag and Adv-Flag-Slc7a5 under the control of the mouse cytomegalovirus (CMV) promoter were packaged by OBiO (Shanghai, China). The adenoviral in vivo delivery method was conducted as previously described [31]. In brief, a 20 μL solution of adenovirus containing 1×10^9 plaque-forming units (pfu) of either Adv-Flag or Adv-Slc7a were delivered from the apex of the left ventricle to the aortic root. A tourniquet was placed around the aorta and the pulmonary artery at a site distal to the tip of the catheter, followed by the injection of the solution. The tourniquet was held in place

for 10 s while the heart pumped against a closed system and then released. To assess the transduction efficiency, the hearts were harvested and sectioned two weeks after transduction, and SLC7A5 expression was detected by Western blots. Hearts were transduced with adenovirus followed by TAC surgery, and were harvested 4 weeks after aortic banding.

Construction of recombinant adeno-associated virus

Recombinant adeno associated virus 9 (rAAV9) packaged by OBiO (Shanghai, China) was used to manipulate the expression of SLC7A5 with a myofibroblast specific promoter Periostin (POSTN) in mouse hearts. A short hairpin RNA (ShRNA) was synthesized, which contained a target sequence for Slc7a5 as follows: GGATCGAGCT GCTCATCATTC. The sequence of scramble as follows: GAAGTCGTGAGAAGTAGAA. 8-week-old wild type male mice (C57BL/6J) were intravenously injected with adeno-associated virus (3×10^{11} v.g./mouse) for three weeks after TAC surgery for one week. The mice were sacrificed four weeks after TAC surgery.

Cell culture, treatment, gene transfer, and plasmid transduction

Neonatal rat cardiac fibroblasts (NRCFs) were isolated from 1- to 3-day-old neonatal Sprague-Dawley rats following established procedures [32]. The cells were plated at a density of 10^6 cells/mL and cultured in Dulbecco's Modified Eagle Medium (DMEM, Invitrogen Corporation, USA) supplemented with 10% Fetal Bovine Serum (FBS) (Biological Industries, Kibbutz Beit Haemek, Israel), and 100 units/mL penicillin and streptomycin (Beyotime Biotechnology, China). The third generation of fibroblasts were placed in serum-free medium for 30 min and subsequently transfected with Adv-Flag (MOI=50) or Adv-Flag-TRIM35 (MOI=50) under the control of the CMV promoter for 6 h. After transfection, the medium containing the adenovirus was replaced with DMEM supplemented with 10% FBS and continued to be cultured for 24 h. Subsequent TGF-β1 (10 ng/mL) treatment experiments were carried out for 24 h.

In Fig. 8, NRCFs were transfected with Adv-Flag (MOI=50) or Adv-Flag-Trim35 (MOI=50) for 24 h, followed by Rapamycin (0.1 μM) administration for 24 h, before the cells were treated with TGF-β1 (10 ng/mL) for 24 h.

Adult mouse primary cardiac fibroblasts (ACFs) were obtained from mice that were 8–10 weeks old. After the atriums and connective tissues were removed, the hearts were finely chopped. The pieces were then broken down for one hour at 37 °C while being shaken with 0.1% type II collagenase (Worthington Biochemical). The cell solution that had been digested was reconstituted in DMEM containing 10% FBS, filtered through a 70 μm filter, and then seeded into a culture dish for additional research.

HEK293T cells, obtained from American type culture collection (ATCC), were cultured in DMEM supplemented with 10% FBS, penicillin and streptomycin. Flag-tagged Trim35, HA-tagged Slc7a5, and His-tagged Ub were purchased from Miaoling (Wuhan, China). For transient transfection, HEK293T cells were transfected with the indicated plasmids by NEOFECT™ DNA transfection reagent according to manufacturer's recommendations.

Procedures of RNA sequencing (RNA-Seq)

A total of eight cardiac tissues were obtained from two distinct cohorts of mice, namely the Sham group and the TAC group. The RNA-Seq processes were performed at GENESKY Co., Ltd, encompassing sample quality assurance, library preparation for transcriptome sequencing, clustering, and sequencing. The identification of differentially expressed genes (DEGs) was performed using the DESeq2 R package (version 1.20.0), with a p-value below the predetermined threshold of 0.05.

HPLC-MS/MS analysis

HPLC-MS/MS analysis was conducted to detect amino acid content in cardiac fibroblasts. Samples were prepared and analyzed using an ExionLC AD system coupled with a QTRAP® 6500+mass spectrometer (Sciex, USA) at Majorbio Bio-Pharm Technology Co. Ltd. (Shanghai, China). Samples were separated using an AdvanceBio MS Spent Media column (2.1×50 mm, 2.7 μm) at 40℃ with a flow rate of 0.5 mL/min and a gradient mobile phase (95% acetonitrile in water with 0.1% formic acid and 10 mM ammonium formate). The chromatographic separation lasted for 6 min with specific gradient conditions. Mass spectrometric data were collected using a UHPLC coupled to a QTRAP® 6500+mass spectrometer (Sciex, USA) operating in positive and negative modes. The LC-MS raw data were analyzed using Sciex software OS, with automatic identification and integration of ion fragments, followed by manual verification. Metabolite concentrations were determined using linear regression standard curves. All samples were stored at 4℃ during analysis.

Immunoprecipitation-mass spectrum (IP-MS)

Cardiac fibroblasts were cultivated on 10-cm plates and subsequently transfected with either Adv-Flag or Adv-Flag-Trim35. Then, the cells were lysed and immunoprecipitated using either anti-IgG or anti-Trim35 antibody. Western blot and silver staining were used to confirm that TRIM35 had been successfully immunoprecipitated. Afterward, the immunoprecipitant protein was used for proteomics analysis using liquid chromatography and tandem mass spectrometry (Lc-Bio Technologies).

Co-immunoprecipitation

The cells were harvested and lysed following previously established protocols [33]. Subsequently, the lysates were incubated overnight at 4 °C with either anti-TRIM35 (sc-100880, Santa Cruz, 1:50) or anti-SLC7A5 (sc-374232, Santa Cruz, 1:50) antibodies. Following this, 30 μL of protein G Agarose beads (Cytiva) were co-incubated with the immune complexes for 4 h at 4 °C. After undergoing three washes with a cold wash buffer and one wash with lysis buffer, the immunoprecipitations were resuspended in 30 μl of lysis buffer and subjected to Western blot analysis to examine the indicated target proteins.

Western blot

Protein extraction was conducted from mouse heart tissues or cultured cells, respectively, followed by immunoblots as previously outlined [33]. In brief, Western blot analyses employed commercially available antibodies: anti-TRIM35 (sc-100880, Santa Cruz, 1:100), anti-GAPDH (AF0006, Beyotime, 1:1000), anti-α-SMA (A17910, abclonal,1:1000), anti-Ub (AF1705, Beyotime, 1:1000), anti-Ub-K63 (ab179434, abcam, 1:1000), anti-HA (AH158, Beyotime, 1:1000), anti-Flag (AF519, Beyotime, 1:1000), p-S6K (AP0564, abclonal, 1:1000), S6K (A2190, abclonal, 1:1000), p-4E-BP1 (AF5806, Beyotime, 1:100), and 4E-BP1 (AG1824, Beyotime, 1:100), followed by incubation with peroxidase-conjugated secondary antibodies. Signal detection utilized the enhanced chemiluminescent (ECL) system (Tanon, China), and densitometry scanning was performed using Image J software. GAPDH was used as the loading control. Results from each experimental group were expressed as relative integrated intensity compared to the control group measured concurrently.

Real-time PCR

Total RNA was extracted as previously described and then converted into cDNA using PrimeScript™ RT Reagent kit with gDNA eraser (Takara RR047A, Japan). Quantitative RT-PCR reactions were performed using the ChamQTM SYBR Color qPCR Master Mix (Vazyme, China) and QuantStudio™ 6 Flex System (Applied Biosystems, USA). HPRT was used as the internal reference for each sample. The primer sequences were showed in in Table S1.

Cardiac fibroblasts proliferation assay

The proliferation of NRCFs was assessed using 5-ethynyl-2-deoxyuridine (EdU) incorporation (Beyotime, C0078S), following established procedures. The proliferative rate of NRCFs was quantified by normalizing the number of EdU-positive cells to the total DAPI-stained cells.

Wound healing assay

The wound healing assay involved the plating of cardiac fibroblasts in 6-well plates, followed by transfection with either adv-Flag or adv-Trim35.Subsequently, the confluent monolayer of cells was subjected to a linear wound area using a 200 μL pipette tip in order to assess the migratory capacity of cardiac fibroblasts. Subsequently, the denuded plate was delicately rinsed to eliminate any disconnected cells. Photographs were taken of cells at the moment of injury and again 24 h following the injury. The calculation of the migratory capability of fibroblasts was performed by measuring the area of wound recovery using the ImageJ software.

Immunofluorescence

The heart tissue chips underwent dewaxing and rehydration, while the cells were fixed using 4% paraformaldehyde. Following these steps, the washed heart tissue chips or cells were permeabilized with 0.1% Triton X-100 and then blocked with 5% normal goat serum (BioGenex, Fremont, CA). Subsequently, they were stained with one or more corresponding antibodies as per the instructions (anti-TRIM35: sc-100880, Santa Cruz, 1:25; anti-Vimentin: D21H3, CST, 1:200; anti-α-SMA: A17910, abclonal,:100; anti-cTnT: ab8295, abcam, 1:200; anti-Collagen III: ab7778, abcam, 1:100; SLC7A5: sc-374232, Santa Cruz antibodies), followed by DAPI (Invitrogen) staining. Afterward, they were incubated with Alexa Fluor® 488 or 594-conjugated secondary antibodies (1:500) (Life Technologies, Carlsbad, CA) at 37 °C for 90 min. For imaging, five fields were randomly selected in each group and captured using a confocal microscope (Zeiss, Germany).

Histological examination

Mouse and human hearts were collected and then immersion-fixed in 4% buffered paraformaldehyde. Subsequently, the heart tissues were embedded in paraffin and cut into 5 μm sections. In brief, all mouse and human heart tissues were counterstained with hematoxylin and eosin (H&E). Additionally, sections of mouse hearts were incubated with the Masson's Trichrome Stain Kit (Solarbio, China).

Wheat germ agglutinin (WGA) staining

The mouse hearts were acquired and preserved in paraffin after being fixed in a 4% buffered formaldehyde solution for a duration of 24 h. The hearts were processed and stained with WGA (G1730, Servicebro, Wuhan, China) using 6-m paraffin-embedded slices, following the manufacturer's protocol. The examination and documentation of the sections were conducted using a fluorescence microscope. The cell membrane was identified by the

presence of green fluorescence, and the surface area of the cardiomyocyte was quantified using Image J software.

Statistics

The data are presented as means ± SD. Statistical analyses were performed using GraphPad Prism 8.0. For comparisons between two groups, an unpaired t-test was conducted. Pearson correlation coefficient (R^2) was performed to assess the correlation between two variables. When comparing more than two groups, one or two-way analysis of variance (ANOVA) was employed, followed by the post hoc Tukey's test. In all cases, $p < 0.05$ was considered statistically significant.

Results

TRIM35 is up-regulated in fibroblasts in murine and human remodeling hearts

First, we investigated in which cells TRIM35 undergoes alterations during the process of cardiac remodeling. Mice were subjected to transverse aortic constriction (TAC) surgical operation for 4 weeks to induce cardiac remodeling. Immunofluorescence staining of heart tissue sections with anti-TRIM35 and anti-Vimentin antibodies, a marker of fibroblasts, revealed strong positive staining of TRIM35 in fibroblasts in the interstitium and blood vessels in TAC-induced mouse hearts (Fig. 1A). Additionally, we co-stained TRIM35 and α-SMA, the marker indicating differentiation from fibroblasts to myofibroblasts, and found that TAC also induced up-regulation of TRIM35 in myofibroblasts (Fig. 1B). However, we did not observe increased co-localization of TRIM35 with the cardiomyocyte marker cTnT in TAC-induced mouse hearts (Fig. 1C). Immunofluorescence staining also demonstrated sporadic expression of TRIM35 in fibroblasts in non-remodeling human heart samples obtained from the patients with double pore type atrial septal defect. However, TRIM35 expression was markedly elevated in fibroblasts within remodeling human heart samples, obtained from excised interventricular septal tissue during surgical on hypertrophic cardiomyopathy (HCM) patients (Fig. 1D). Consistently, isolation of fibroblasts from fibrotic cardiac tissues and subsequent Western blot analysis revealed a significant up-regulation of TRIM35 in cardiac fibroblasts (Fig. 1E). To elucidate the stimulus to which TRIM35 responds during pressure overload-induced ventricular remodeling, we first conducted a correlation analysis to investigate the relationship between Trim35 gene expression and the classical fibrotic activation signal TGF-β1. The RNA-Seq dataset GSE1133054 was downloaded from the Gene Expression Omnibus database, and we subsequently examined the correlation between Trim35 and TGFB1 gene expression in the hearts of HCM patients. As predicted, Trim35 gene level showed significant positive correlation with the expression level of TGFB1 gene in the hearts of HCM patients (Fig. 1F). Furthermore, we stimulated neonatal rat ventricular fibroblasts (NRCFs) with TGF-β1 (10 ng/mL), and Western blot analysis showed a significant induction of TRIM35 and α-SMA expression (Fig. 1G), suggesting TRIM35 is a novel target responsive to TGF-β1 in NRCFs. These data suggest that TRIM35 expression is up-regulated in activated fibroblasts induced by pressure overload and can respond to TGF-β1 stimulus.

Fibroblast-specific deletion of TRIM35 ameliorates cardiac fibrosis

Next, we investigated the potential function of TRIM35 in fibroblasts during the process of cardiac fibrosis. Fibroblast-specific Trim35 gene knockout ($Trim35^{cKO}$) mice were created by crossing $Trim35^{f/f}$ mice with $Col1a2\text{-}Cre^{ERT}$ mice and treated with 50 mg/kg/day of tamoxifen for 5 days (Fig. S2A-C). Masson's trichrome staining showed that both myocardial interstitial and perivascular collagen deposition caused by TAC surgery were obviously ameliorated in the $Trim35^{cKO}$ mice (Fig. 2A, B). We further examined the changes in the expression of fibrosis-related genes in $Trim35^{cKO}$ mouse hearts. TRIM35 specific deficiency in fibroblasts significantly reduced the TAC-induced up-regulation of Col1a1, Col3a1, and Tgfb1 mRNA levels (Fig. 2C-E). Additionally, immunofluorescence staining of heart tissue sections with anti-α-SMA antibody revealed a significant reduction in positive staining in the TAC-induced $Trim35^{cKO}$ mouse myocardium, compared to their littermate controls (Fig. 2F). Increased protein expression of α-SMA was also detected in the cardiac fibroblasts isolated from TAC-induced $Trim35^{f/f}$ mouse heart tissues, but reduced in TAC-induced $Trim35^{cKO}$ mouse heart tissues (Fig. 2G). Next, we examined the cardiac function of the mice. Echocardiographic analysis showed that the absence of TRIM35 in fibroblasts improved the cardiac function deterioration induced by TAC surgery, as evidenced by the up-regulation of EF% and FS% (Fig. 2H, I). Notably, TAC surgery did not induce significant cardiac dysfunction and fibrosis in $Trim35^{cKO}$ mice, suggesting that TRIM35 specific deficiency in fibroblasts can resist remodeling-related pathomorphological changes in response to pressure overload (Fig. 2). Collectively, these data elucidate that fibroblast-specific knockout of Trim35 improves pressure overload-induced cardiac fibrosis and cardiac function.

Fibroblast-specific deletion of TRIM35 improves cardiac hypertrophy

Excessive fibrosis can lead to the hardening and thickening of myocardial tissue, thereby affecting the structure and function of the myocardium [2]. We then examined the effect of TRIM35 on cardiac hypertrophy. TAC-mice

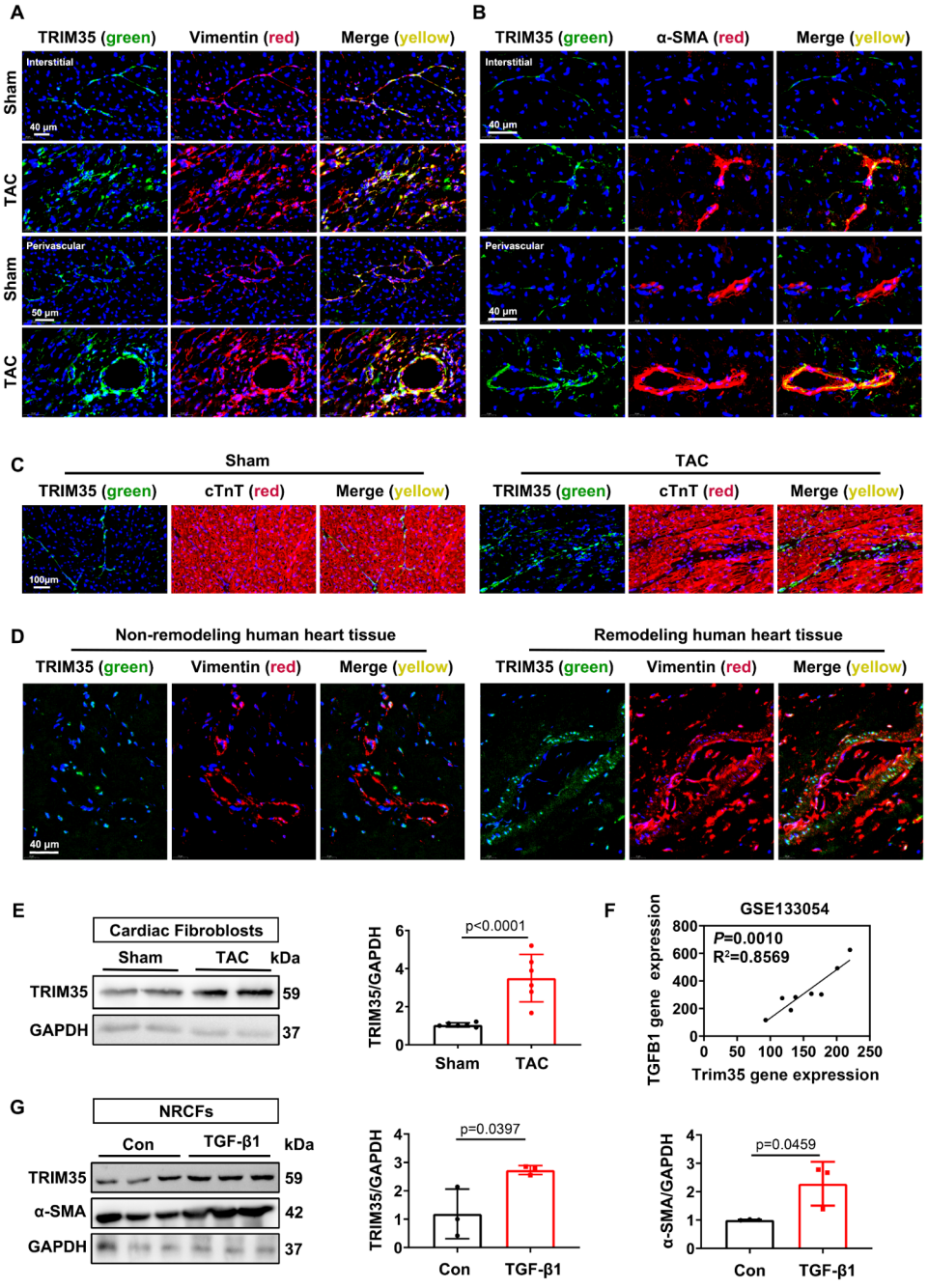

Fig. 1 TRIM35 is up-regulated in fibroblasts in fibrotic heart tissues. 8-week-old male mice were subjected to Sham or TAC surgery, and heart tissues were harvested 4 weeks post-surgery. **A** Immunofluorescence co-staining for Vimentin (red) with TRIM35 (green) and DAPI (blue) in the mouse heart tissue sections. $n=6$. **B** Immunofluorescence co-staining for α-SMA (red) with TRIM35 (green) and DAPI (blue) in the mouse heart tissue sections. $n=6$. **C** Immunofluorescence co-staining for cTnT (red) with TRIM35 (green) and DAPI (blue) in the mouse heart tissue sections. $n=6$. **D** Immunofluorescence co-staining for Vimentin (red) with TRIM35 (green) and DAPI (blue) in the human heart tissue sections. $n=4$. **E** Representative Western blot analysis was performed to assess the protein level of TRIM35 in cardiac fibroblasts isolated from the hearts of mice subjected to Sham or TAC surgery for 4 weeks, and corresponding statistic of TRIM35 was shown. $n=6$. **F** Pearson correlation coefficients between Trim35 mRNA level and TGFB1 mRNA level in human hearts with HCM. **G** Representative Western blots and statistical results of TRIM35 and α-SMA in NRCFs treated with TGF-β1 (10 ng/mL). $n=3$. Data are presented as mean ± SD. The data shown in **E** and **G** were analyzed using an unpaired t-test

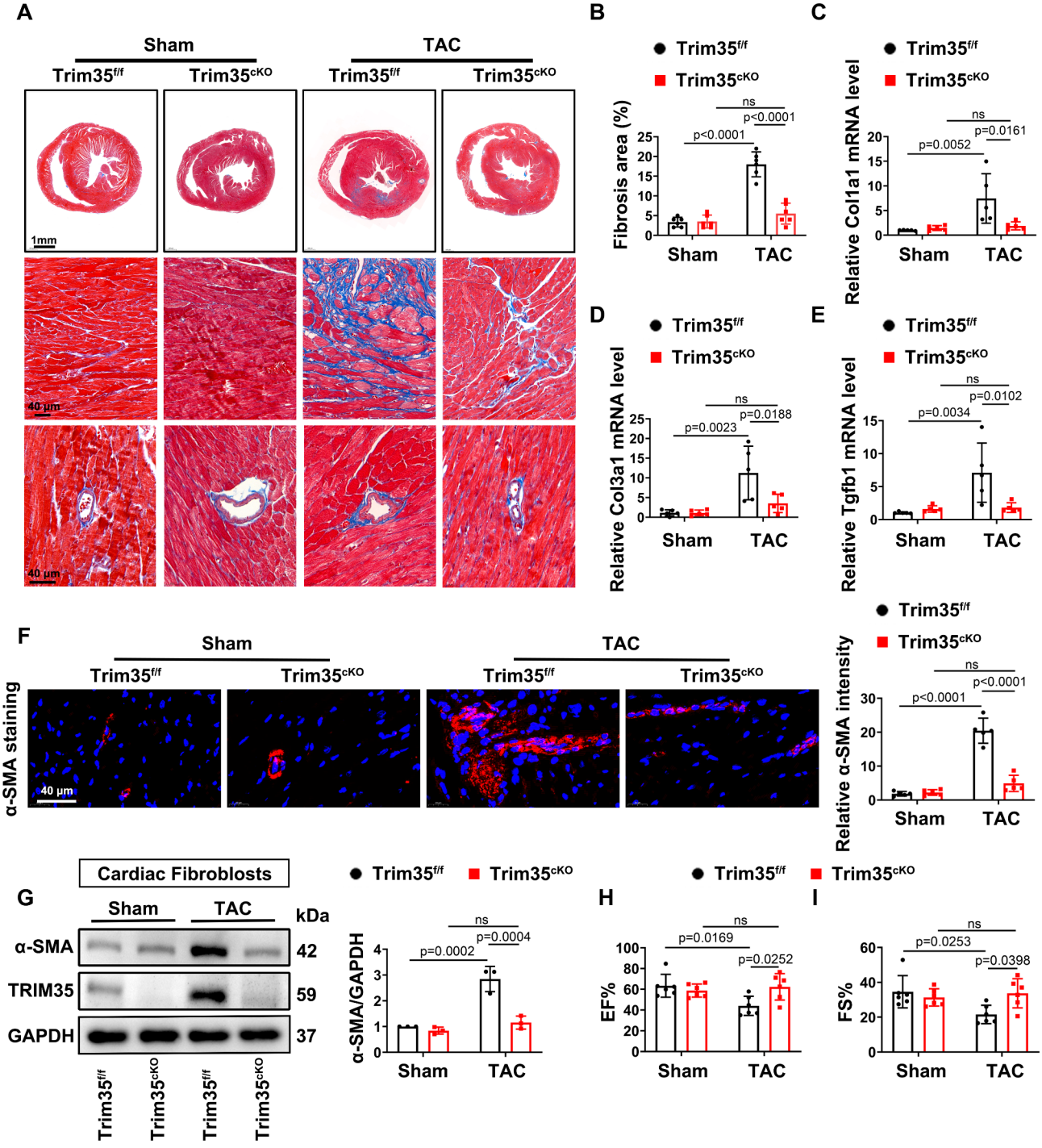

Fig. 2 Fibroblast-specific deletion of TRIM35 ameliorates TAC-induced cardiac fibrosis. 8-week-old Trim35$^{f/f}$ and Trim35^{cKO} male mice were subjected to Sham or TAC surgery, and heart tissues were harvested 4 weeks post-surgery. **A**, **B** Masson's trichrome staining was performed to detect myocardial interstitial and perivascular collagen deposition, and the corresponding statistical result of fibrosis was shown. $n = 6$. **C-E** The mRNA levels of Collagen Ia1 (Col 1a1), Collagen IIIa1 (Col 3a1), and Tgfb1. All normalized to HPRT. $n = 5$. **F** Fibroblast differentiation was analyzed by immunofluorescence staining with anti-α-SMA antibody (red) and DAPI (blue), and the statistical result of relative α-SMA intensity was shown. $n = 5$. **G** Representative Western blots and statistical result of α-SMA in cardiac fibroblasts isolated from mouse hearts. $n = 3$. **H**, **I** Quantification of echocardiographic parameters of ejection fraction (EF%) and fractional shortening (FS%). $n = 6$. Data are presented as mean ± SD. The data were analyzed using two-way ANOVA corrected by the post hoc Turkey's test

with a specific deficiency of TRIM35 in fibroblasts displayed a smaller heart size, and the lower ratio of heart weight (HW)/body weight (BW) (Fig. 3A, B). Echocardiographic analysis showed that TAC dramatically increased interventricular septum thickness (IVS) and left ventricular (LV) posterior wall thickness (LVPW) in Trim35$^{f/f}$ mice. However, these parameters were significantly decreased in Trim35^{cKO}-TAC-mice (Fig. 3C-F). H&E and WGA staining showed that the cardiac myocyte cross-sectional area was decreased by Trim35 gene conditional deletion in TAC-mice (Fig. 3G). Consistent with the morphological phenotypes in Trim35^{cKO}-TAC-mice, the expression of hypertrophic-related genes such as atrial natriuretic peptide (ANP), brain natriuretic peptide (BNP) and β-myosin heavy chain (β-MHC) were also accordingly down-regulated (Fig. 3H-J). Although fibroblast-specific deletion of TRIM35 improves pressure overload-induced cardiac hypertrophy compared to their littermate controls, a moderate increase in IVS; s, LVPW; s, cell size, and mRNA expression of ANP and β-MHC was also observed in the hearts of Trim35^{cKO} mice subjected to TAC surgery (Fig. 3C, E, G, H and J), which showed a compensated hypertrophy also established in Trim35^{cKO} mice in response to pressure overload. These

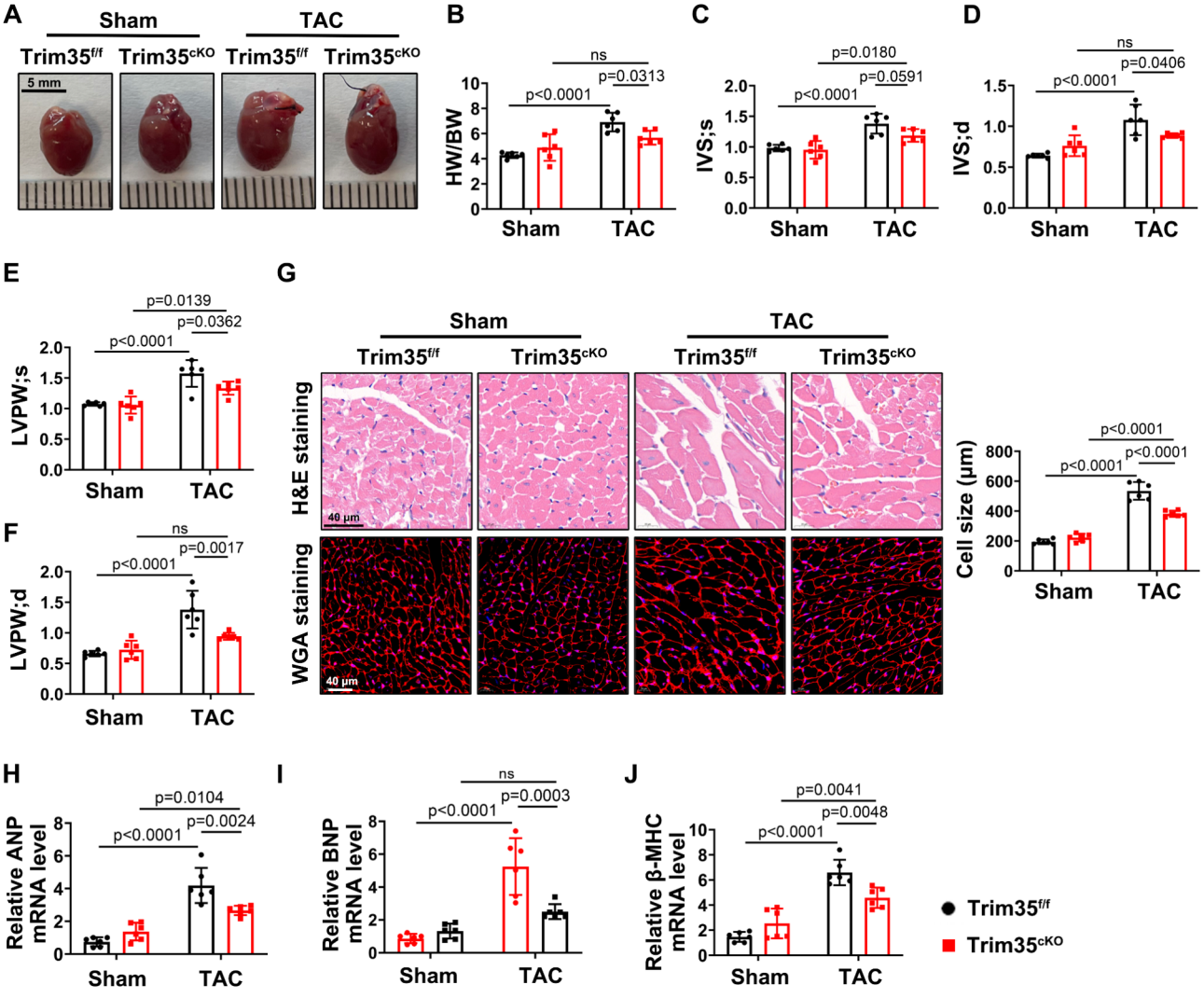

Fig. 3 Fibroblast-specific deletion of TRIM35 protects against TAC-induced cardiac hypertrophy. 8-week-old Trim35$^{f/f}$ and Trim35^{cKO} male mice were subjected to Sham or TAC surgery, and heart tissues were harvested 4 weeks post-surgery. **A** Representative gross appearance of whole hearts. **B** The ratio of HW/BW. heart weight (HW), body weight (BW). $n = 6$. **C-F** Quantification of echocardiographic parameters includes interventricular septum systolic dimension (IVS; s), interventricular septum diastolic dimension (IVS; d), left ventricle posterior wall thickness systole (LVPW; s), and left ventricle posterior wall thickness diastole (LVPW; d). $n = 6$. **G** Hematoxylin and eosin (H&E) and Wheat germ agglutinin (WGA) staining were performed to detect cardiomyocyte cross-sectional area, and the statistical result of cell size was shown. $n = 6$. **H-J** The mRNA expression of ANP, BNP, and β-MHC were analyzed by qRT-PCR. Atrial natriuretic peptide (ANP), brain natriuretic peptide (BNP), β-myosin heavy chain (β-MHC). All normalized to HPRT. $n = 6$. Data are presented as mean ± SD. The data were analyzed using two-way ANOVA corrected by the post hoc Turkey's test

data suggest that a specific deficiency of TRIM35 in fibroblasts also alleviates cardiac hypertrophy.

Overexpression of TRIM35 activates cardiac fibroblasts and induces cardiomyocyte hypertrophy

TGF-β1 is a potent inducer of cardiac fibrosis and hypertrophy. Next, we validated the effect of TRIM35 on cardiac fibroblast activation in vitro. Wound healing assay revealed that overexpression of TRIM35 promoted the migration of fibroblasts induced by TGF-β1 (Fig. 4A). EdU staining demonstrated that TRIM35 enhanced the proliferation of fibroblasts after TGF-β1 administration (Fig. 4B). Additionally, α-SMA fluorescence staining and Western blots indicated that the up-regulation of TRIM35 expression significantly promoted TGF-β1-induced transdifferentiation of fibroblasts (Fig. 4C, D). Consistently, overexpression of TRIM35 also augmented TGF-β1-induced increase in the mRNA levels of Col1a1, Col3a1, Periostin (POSTN) and Fibronectin (Fn) in fibroblasts (Fig. 4E-H). It is worth noting that overexpression of TRIM35 can activate fibroblasts under physiological conditions (Fig. 4A-H). To investigate how fibroblast-specific loss of TRIM35 regulates the process of cardiac hypertrophy, we used the conditioned media collected from the TRIM35-overexpressed cardiac fibroblasts and the virus control group to treat cardiomyocytes. Figure 4I-L demonstrate that conditioned medium from TRIM35-overexpressing NRCFs strongly induced hypertrophy in neonatal rat cardiac myocytes (NRCMs), as evidenced by a significant increase in cardiomyocyte surface area and the up-regulation of hypertrophy-related genes ANP, BNP, and β-MHC (Fig. 4I-L). Collectively, these data indicate that TRIM35 activates cardiac fibroblasts and facilitates the transmission of pro-hypertrophic signals derived from cardiac fibroblasts to cardiomyocytes.

SLC7A5 is a target of TRIM35 and a key factor in suppressing cardiac fibrosis

To explore the molecular mechanism by which TRIM35 regulates fibroblast activation, we utilized RNA-Seq and IP-MS to screen for potential targets. RNA-Seq data revealed that SLC7A5 is among the top 50 differentially expressed genes (DEGs) in wild-type mice undergoing TAC-induced cardiac remodeling, compared to Sham-operated mice. Notably, SLC7A5 is the only molecule among the top 50 DEGs that was also detected in the immunoprecipitate of TRIM35 in cultured NRCFs transfected with Adv-Trim35 (Fig. 5A-C, Fig. S3). These findings suggest that SLC7A5 not only interacts with TRIM35 in NRCFs but may also play a critical role in the response to pressure overload. The up-regulated protein expression of SLC7A5 in TAC-induced fibrotic mouse hearts was confirmed by Western blot analysis (Fig. 5D). Additionally, the RNA-Seq dataset GSE1133054 revealed a significant up-regulation of Slc7a5 mRNA levels in the hearts of patients with HCM exhibiting adverse ventricular remodeling (Fig. 5E). To further demonstrate in vivo that SLC7A5 serves as a key regulator of cardiac fibrosis, we established myofibroblast-specific Slc7a5 knockdown mice by administering rAAV9-Postn-ShSlc7a5 via tail vein injection one week after TAC surgery, and the mice were sacrificed four weeks after TAC surgery. Western blot results indicated that administration of rAAV9-Postn-ShSlc7a5 reduced SLC7A5 protein level by approximately 76% in TAC-induced mice hearts (Fig. 5F). Masson's trichrome staining showed that both myocardial interstitial and perivascular collagen deposition caused by TAC surgery were obviously ameliorated in the Slc7a5- knockdown mouse hearts (Fig. 5G, H). Echocardiographic analysis revealed that down-regulation of SLC7A5 in myofibroblasts mitigated the cardiac function deterioration induced by TAC surgery, as indicated by increased EF% and FS% (Fig. 5I). These results suggest that SLC7A5 is not only a potential target of TRIM35 but also a key factor in inhibiting the progression of cardiac fibrosis.

TRIM35 up-regulates SLC7A5 protein level in cardiac fibroblasts involving K63-linked ubiquitination

Furthermore, we investigated the molecular mechanisms by which TRIM35 regulates SLC7A5 expression level. Interestingly, The RNA-Seq dataset GSE133054 revealed that there was no correlation between Trim35 and Slc7a5 gene expression in human hearts with HCM (Fig. 6A). The mRNA level of Slc7a5 was elevated in TAC-induced $Trim35^{cKO}$ mouse hearts but remained unaffected by the conditional deletion of the Trim35 gene (Fig. 6B). Consistently, the mRNA level of Slc7a5 was also unaffected by TRIM35 overexpression in cultured NRCFs (Fig. 6C). These results indicated that TRIM35 does not regulate the transcriptional level of SLC7A5. However, the TRIM35 protein level showed a significant positive correlation with the SLC7A5 protein level in remodeling mouse hearts (Fig. 6D). Additionally, we found that TRIM35 specific deficiency in fibroblasts significantly reduced the TAC-induced up-regulation of SLC7A5 protein, and overexpression of TRIM35 significantly increased the protein level of SLC7A5 in cultured NRCFs (Fig. 6E, F). These data suggest that TRIM35 may influence the post-translational level of SLC7A5. To examine the direct interaction between TRIM35 and SLC7A5, protein structure docking was performed and predicted a direct binding between them (Fig. 6G). Consistently, Co-IP was performed to demonstrate the interaction between TRIM35 and SLC7A5 in NRCFs (Fig. 6H). Given that TRIM35 is an E3 ubiquitin ligase capable of ubiquitinating substrate proteins, thereby affecting their protein stability, we then examined the effect of

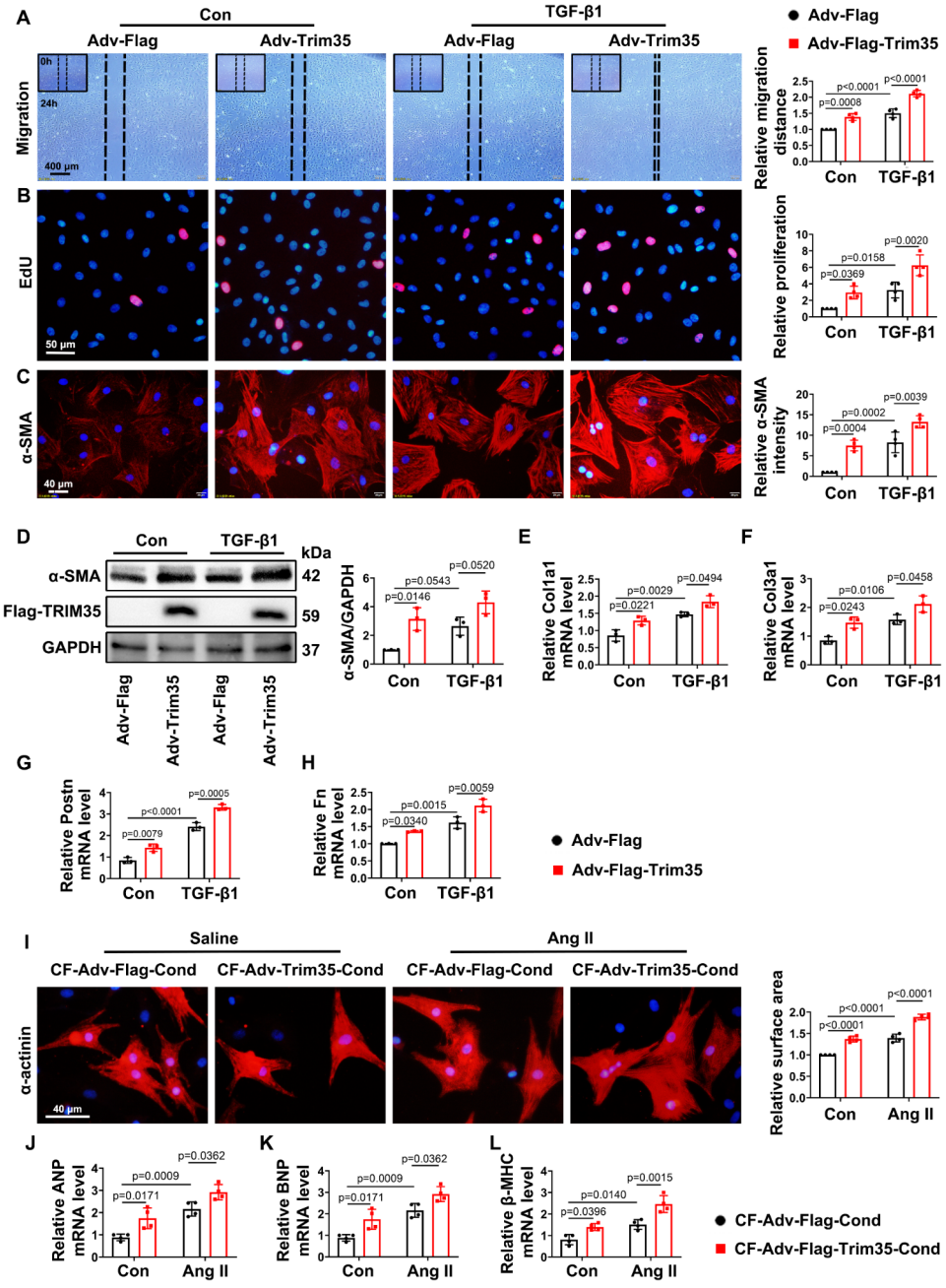

Fig. 4 Overexpression of TRIM35 activates cardiac fibroblasts and induces cardiomyocyte hypertrophy in vitro. Neonatal rat cardiac fibroblasts (NRCFs) were isolated from 1 to 3-day-old neonatal Sprague-Dawley rats, and transfected with Adv-Trim35 or Adv-Flag for 48 h before being treated with TGF-β1 (10 ng/mL) for 24 h. **A** The wound healing assay was performed to detect the migration distance of NRCFs, and the statistical result of relative migration distance was shown. $n = 4$. **B** Representative images showing EdU (red) localization of each group indicated the proliferative ability of NRCFs, and nuclei were stained with DAPI (blue). The statistical result of relative proliferation was shown. $n = 4$. **C** NRCFs were stained with anti-α-SMA ((red) antibody, and nuclei were stained with DAPI (blue). The statistical result of relative α-SMA intensity was shown. $n = 4$. **D** Representative Western blots and statistical result of α-SMA in NRCFs. $n = 3$. **E-H** The relative mRNA levels of Col1a1, Col3a1, Postn, and Fn. $n = 3$. **I** The conditioned media collected from the TRIM35-overexpressed NRCFs (CF-Adv-Trim35-Cond) or the virus control group (CF-Adv-Flag-Cond) to stimulate neonatal cardiac myocytes (NRCMs) treated with Ang II (1 μM) or saline. Cardiomyocyte surface areas were analyzed by immunofluorescence staining with anti-α-actinin antibody (red) and DAPI (blue), and the statistical result of relative surface area was shown. $n = 4$. **J-L** The mRNA expression of ANP, BNP, and β-MHC were analyzed by qRT-PCR. All normalized to HPRT. $n = 4$. Data are presented as mean ± SD. The data were analyzed using two-way ANOVA corrected by the post hoc Turkey's test

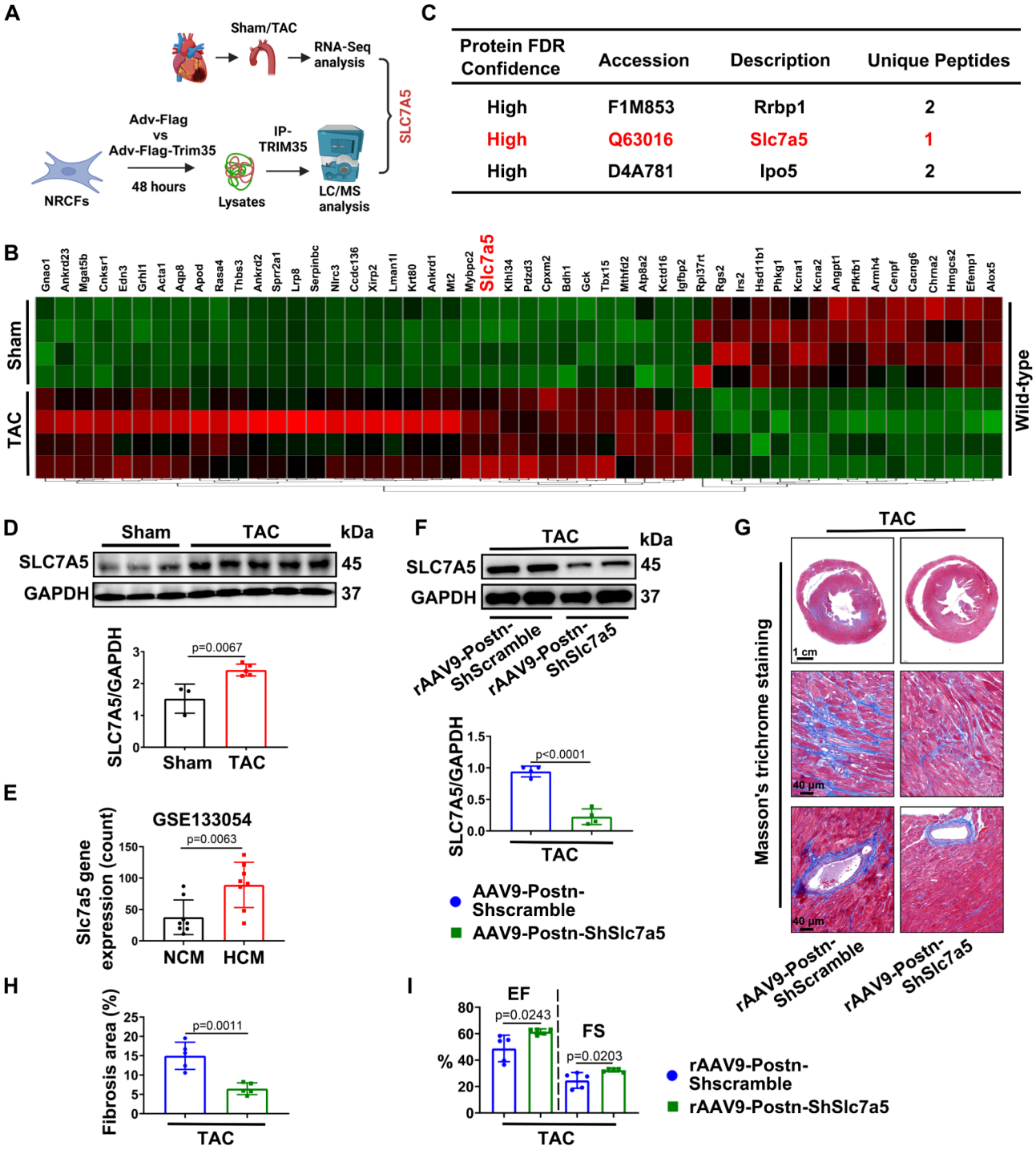

Protein FDR Confidence	Accession	Description	Unique Peptides
High	F1M853	Rrbp1	2
High	Q63016	Slc7a5	1
High	D4A781	Ipo5	2

Fig. 5 SLC7A5 is identified as a target of TRIM35 and suppression of its expression in myofibroblasts alleviates cardiac fibrosis. **A** Treatment regimen. **B** 8-week-old wild-type male mice were subjected to Sham or TAC surgery, and heart tissues were harvested 4 weeks post-surgery. RNA-Seq analysis revealed alterations in the top 50 differentially expressed genes (DEGs) in TAC-induced mouse hearts. $n=4$. **C** NRCFs were transfected with Adv-Flag or Adv-TRIM35 for 48 h, after which the cells were harvested for immunoprecipitation using an anti-TRIM35 antibody. LC-MS analysis was conducted to identify target proteins that may interact with TRIM35. **D** Representative Western blots and statistical result of SLC7A5 in Sham or TAC-induced mouse hearts. $n=3$, and 5, respectively. **E** The Slc7a5 mRNA level in the human hearts with HCM, and the data was obtained from RNA-Seq dataset GSE1133054. **F** Myofibroblast-specific Slc7a5 knockdown mice were established by administering rAAV9-Postn-ShSlc7a5 via tail vein injection one week after TAC surgery, and the mice were sacrificed four weeks after TAC surgery. Representative Western blots and statistical result of SLC7A5 in mouse hearts. $n=4$. **G**, **H** Masson's trichrome staining was performed to detect myocardial interstitial and perivascular collagen deposition, and the corresponding statistical result of fibrosis was shown. $n=5$. **I** Quantification of echocardiographic parameters of EF% and FS%. $n=5$. Data are presented as mean ± SD. The data were analyzed using an unpaired t-test

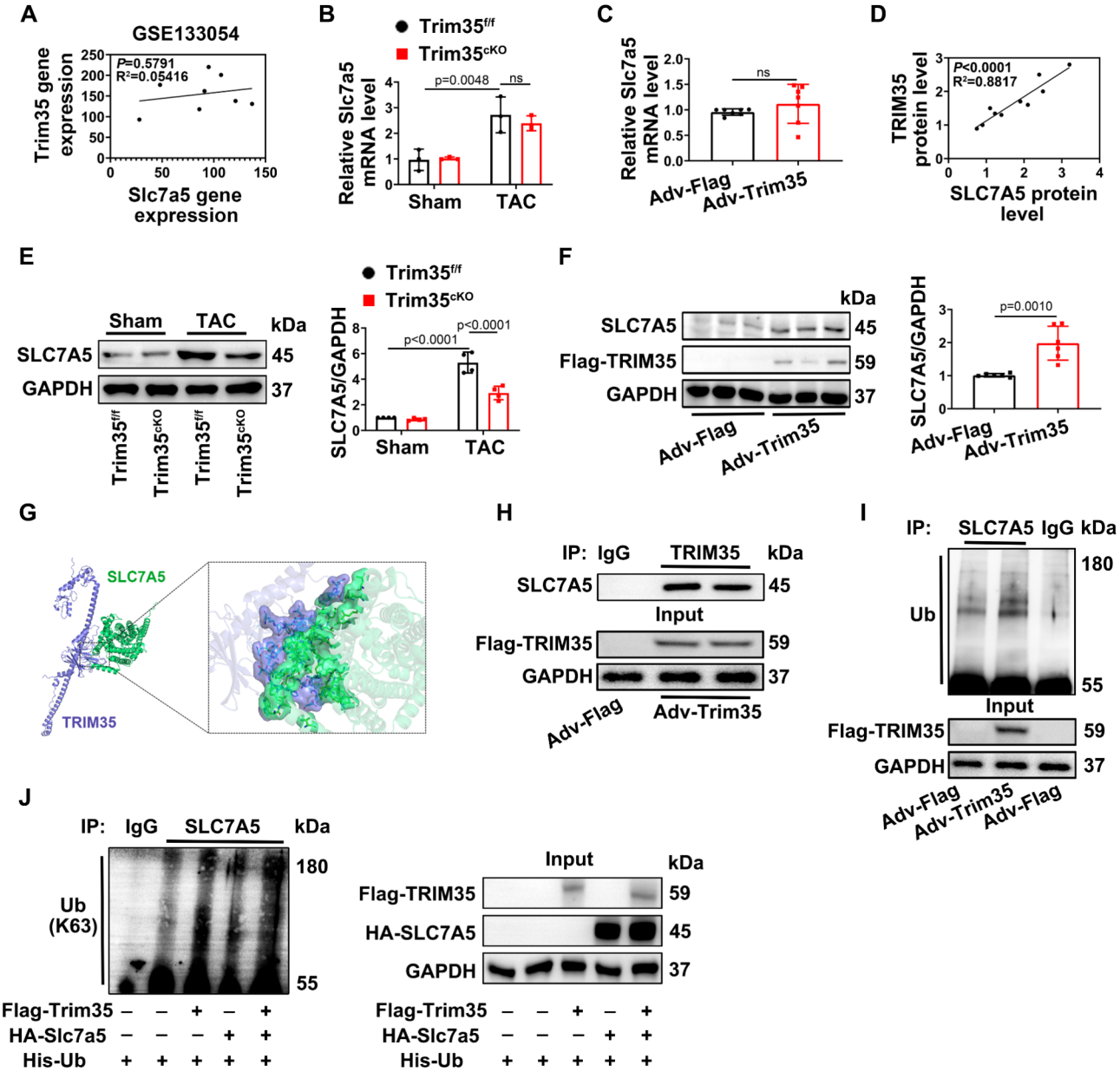

Fig. 6 TRIM35 augments SLC7A5 protein level in cardiac fibroblasts involving K63-linked ubiquitination. **A** Pearson correlation coefficients between Slc7a5 mRNA level and Trim35 mRNA level in human hearts with HCM were calculated, and the data was obtained from RNA-Seq dataset GSE1133054. **B** The mRNA level of Slc7a5 was analyzed by qRT-PCR in mouse hearts. Normalized to HPRT. $n=3$. **C** The mRNA expression of Slc7a5 was analyzed by qRT-PCR in NRCFs transfected with Adv-Flag or Adv-Trim35 for 48 h. All normalized to HPRT. $n=7$. **D** Pearson correlation coefficients between SLC7A5 protein level and TRIM35 protein level in remodeling mice hearts. **E** Representative Western blots and statistical result of SLC7A5 in mouse hearts. $n=4$. **F** Representative Western blots and statistical result of SLC7A5 in NRCFs transfected with Adv-Flag or Adv-Trim35 for 48 h. $n=6$. **G** The structure of TRIM35 and SLC7A5 protein were built using AlphaFold2, and the interaction between them was predicted by ZDOCK. Docking Score = -377.2. **H** Interaction of TRIM35 with SLC7A5 in NRCFs transfected with Adv-Flag or Adv-Trim35 for 48 h was determined by co-immunoprecipitation with anti-TRIM35 antibody followed by immunoblot with anti-SLC7A5 antibody. IgG as a negative control. $n=3$. **I** NRCFs were transfected with Adv-Flag or Adv-Trim35 for 48 h. Immunoprecipitation with the antibody against SLC7A5, and followed by immunoblot with anti-Ub antibody. IgG as a negative control. $n=3$. **J** HEK293T cells transduced with His-Ub, HA-Slc7a5, and Flag-Trim35 vectors were immunoprecipitated with the antibody against SLC7A5, and followed by immunoblot with anti-Ub-K63 antibody. IgG as a negative control. $n=3$. Data are presented as mean ± SD. The data shown in **B**, **E** were analyzed using two-way ANOVA corrected by the post hoc Turkey's test, and shown in **C**, **F** were analyzed using an unpaired t-test

TRIM35 on the ubiquitination modification of SLC7A5 [19]. As expected, Fig. 6I showed that overexpression of TRIM35 significantly increased the ubiquitination level of SLC7A5 in NRCFs (Fig. 6I). It has been reported that TRIM35 catalyzes K63-linked ubiquitination of targets, and K63-mediated ubiquitination enhances the stability and activity of substrates [14]. HEK293T cells transduced with His-Ub, HA-Slc7a5, and Flag-Trim35 vectors were immunoprecipitated with the antibody against SLC7A5, and followed by immunoblot with anti-Ub-K63 antibody. Co-transduction with His-Ub, HA-Slc7a5, and Flag-Trim35 plasmids increased K63-linked polyubiquitination (Fig. 6J). These findings suggest that TRIM35 up-regulates SLC7A5 protein level in cardiac fibroblasts at least partially through K63-linked ubiquitination.

TRIM35 promotes amino acid transport and activates the mTORC1 signaling in fibroblasts

SLC7A5 is a critical amino acid transporter, playing a key role in transporting amino acids, from the extracellular environment into the cell across the cell membrane, which activates mTORC1 signaling [28]. Next, we further examined whether targeting SLC7A5 with TRIM35 affects the amino acid content in fibroblasts. Figure 7A demonstrated that overexpression of TRIM35 in NRCFs increased the amino acid content of 13 out of 20 amino acids ($p<0.05$), with 2 showing a p-value of less than 0.01 (Fig. 7A). Additionally, overexpression of TRIM35 activated the mTORC1 signaling pathway in a physiological state, as evidenced by increased p-S6K and p-4E-BP1 levels. Furthermore, we also observed that overexpression of TRIM35 further up-regulated the phosphorylation level of S6K and 4E-BP1 in NRCFs following TGF-β1 administration (Fig. 7B). To determine whether fibroblast-specific deletion of TRIM35 inhibits the activation of the mTORC1 signaling pathway in vivo, we assessed the protein levels of p-S6K and p-4E-BP1 in mouse heart tissues. Western blot analysis revealed that the TAC-induced an increase in p-S6K and p-4E-BP1 levels was significantly inhibited in the heart tissues of $Trim35^{cKO}$ mice (Fig. 7C). Accordingly, we claimed that TRIM35 enhances amino acid transport in fibroblasts and activates the mTORC1 signaling pathway, contributing to the increased protein synthesis associated with fibroblast activation.

mTORC1 signaling is crucial for the regulatory role of TRIM35 in TGF-β1-induced fibroblast activation

Next, we aimed to determine whether TRIM35-induced fibroblast activation was mediated by the activation of the mTORC1 signaling pathway, using Rapamycin, an mTORC1 inhibitor. NRCFs were transfected with Adv-Flag or Adv-Trim35 for 24 h, followed by treatment with Rapamycin (0.1 μM) for 24 h, and then exposed to TGF-β1 for an additional 24 h. Western blots indicated that Rapamycin applied at 0.1 μM significantly inhibited mTORC1 signaling as evidenced by lower protein level of p-S6K and p-4E-BP1 (Fig. 8A). The wound healing assay showed that overexpression of TRIM35 did not effectively enhance the migration of fibroblasts induced by TGF-β1 when Rapamycin was administered (Fig. 8B). EdU staining demonstrated that while TRIM35 increased fibroblast proliferation following TGF-β1 administration, there was a significant reduction in EdU-positive cells co-stained with DAPI in Rapamycin-treated NRCFs (Fig. 8C). Additionally, α-SMA fluorescence staining indicated that mTORC1 inhibition suppressed the transdifferentiation of fibroblasts induced by TRIM35 overexpression in TGF-β1-treated NRCFs (Fig. 8D). Consistently, mTORC1 inhibition also diminished the TRIM35 overexpression-induced increase in the mRNA levels of Col1a1, Col3a1, and Postn in TGF-β1-treated fibroblasts (Fig. 8E-G). These findings suggest that mTORC1 signaling is crucial for the regulatory role of TRIM35 in TGF-β1-induced fibroblast activation.

TRIM35 triggers cardiac fibrosis via SLC7A5

To investigate whether TRIM35 regulates ventricular remodeling through SLC7A5, we transfected mouse hearts with an adenovirus expressing SLC7A5 via intracardiac injection [31]. One week after intracardiac injection of Adv-Slc7a5 in wild-type mouse hearts, a significant increase in SLC7A5 protein level was observed in the left ventricular myocardium (Fig. S4A, B). Immunofluorescence staining of heart tissue sections with anti-TRIM35 and anti-Vimentin or anti-cTnT antibodies revealed stronger positive SLC7A5 staining in fibroblasts and cardiomyocytes within heart tissues overexpressing SLC7A5 (Fig. S4C). In contrast, no significant differences were observed in the liver, spleen, lung, or kidney (Fig. S4D), which indicates that transfection of mouse hearts with an adenovirus expressing SLC7A5 via intracardiac injection is heart-specific. Next, the $TRIM35^{f/f}$ and $TRIM35^{cKO}$ mice transfected with Adv-Flag or Adv-Slc7a5 for one week underwent Sham or TAC surgery for 4 weeks (Fig. 9A, S4E). Figure S4F showed that transfection with Adv-Slc7a5 for one week did not affect the cardiac function of $TRIM35^{f/f}$ and $TRIM35^{cKO}$ mice without surgery, as indicated by similar EF% and FS% values (Fig. S4F). Furthermore, overexpression of SLC7A5 in the myocardium did not affect cardiac function, hypertrophy, or fibrosis in mice that underwent sham surgery for 4 weeks (Fig. S4G, H). In TAC-induced mice, Masson's trichrome and Col3 staining revealed that overexpression of SLC7A5 significantly reversed the reduction in fibrosis area caused by conditional knockout of the Trim35 gene (Fig. 9B-C). Consistently, while Trim35 conditional knockout suppressed the mRNA levels of fibrosis-related genes Col1a1, Col3a1, and Tgfb1, overexpression

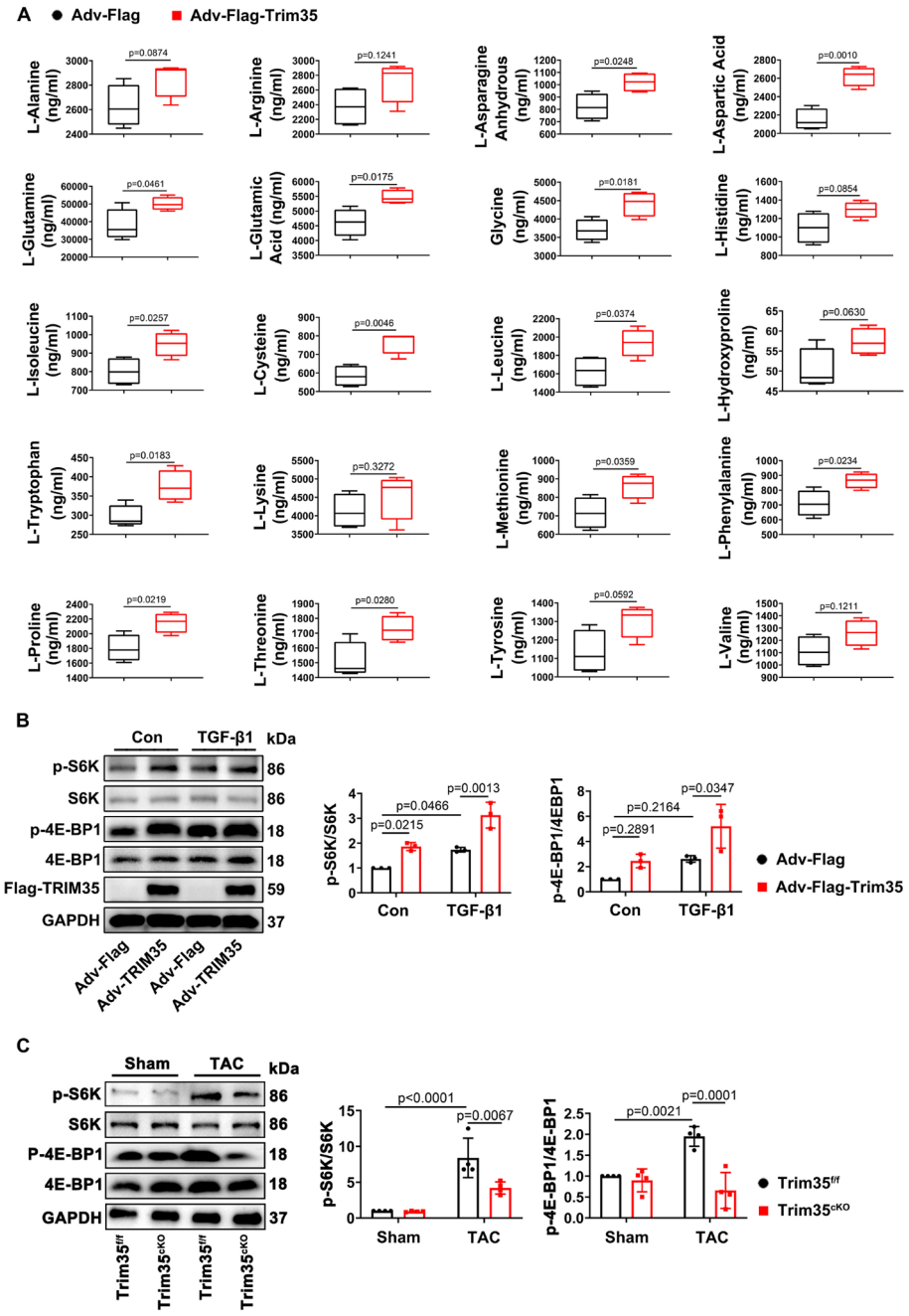

Fig. 7 TRIM35 promotes amino acid transport and activates the mTORC1 signaling. **A** NRCFs were transfected with Adv-Trim35 or Adv-Flag for 48 h. HPLC-MS/MS analysis was performed to detect the content of amino acid in NRCFs. $n = 4$. **B** NRCFs were transfected with Adv-Trim35 or Adv-Flag for 48 h before the cells were treated with TGF-β1 (10 ng/mL) for 24 h. Representative Western blots and statistical results of p-S6K and p-4E-BP1 in NRCFs. $n = 3$. **C** Representative Western blots and statistical results of p-S6K and p-4E-BP1 in mouse hearts. $n = 4$. Data are presented as mean ± SD. The data shown in **A** were analyzed using an unpaired t-test, and shown in **B**, **C** were analyzed using two-way ANOVA corrected by the post hoc Turkey's test

of SLC7A5 significantly increased the mRNA levels of these genes (Fig. 9D-F). Immunofluorescence staining with anti-α-SMA antibody in TAC-induced TRIM35^{cKO} mouse hearts revealed reduced fibroblast differentiation, whereas overexpression of SLC7A5 enhanced fibroblast differentiation (Fig. 9G). Echocardiographic analysis showed that fibroblast-specific deletion of TRIM35 increased EF% and FS% in mice subjected to TAC surgery, but it did not confer additional protection when SLC7A5 was overexpressed (Fig. 9H, I).

To further investigate whether the regulatory mechanism of TRIM35 on pressure overload-induced myocardial fibrosis depends on SLC7A5, we assessed the ubiquitination modification of SLC7A5 and the activation

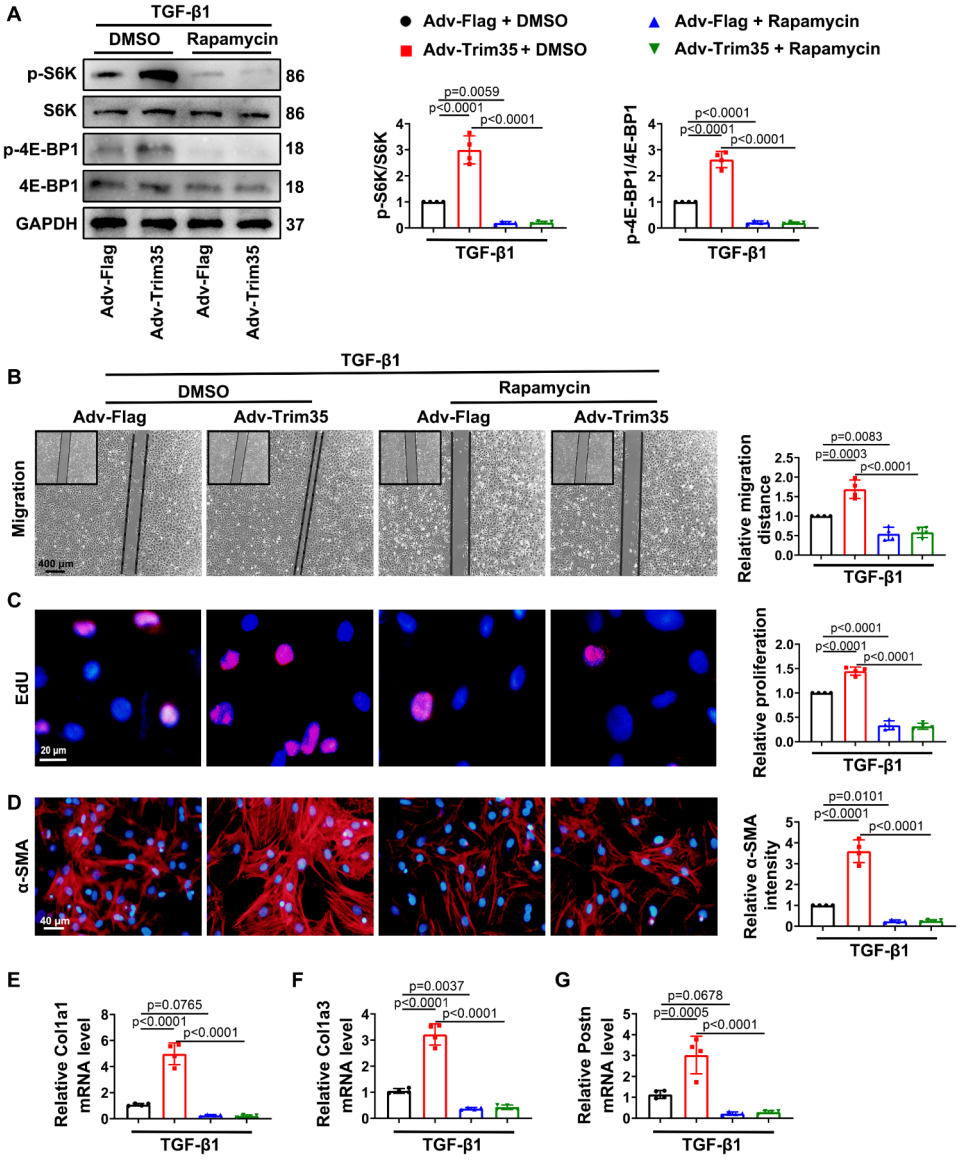

Fig. 8 Inhibition of mTORC1 reverses the TRIM35 overexpression-mediated activation of NRCFs treated by TGF-β1. NRCFs were transfected with Adv-Flag or Adv-Trim35 for 24 h, followed by treatment with Rapamycin (0.1 μM) for 24 h, and then exposed to TGF-β1 (10 ng/mL) for an additional 24 h. **A** Representative Western blots and statistical results of p-S6K and p-4E-BP1 in NRCFs. $n = 4$. **B** The wound healing assay was performed to detect the migration distance of NRCFs, and the statistical result of relative migration distance was shown. $n = 4$. **C** Representative images showing EdU (red) localization of each group indicated the proliferative ability of NRCFs, and nuclei were stained with DAPI (blue). The statistical result of relative proliferation was shown. $n = 4$. **D** NRCFs were stained with anti-α-SMA ((red) antibody, and nuclei were stained with DAPI (blue). The statistical result of relative α-SMA intensity was shown. $n = 4$. **E-G** The relative mRNA levels of Col1a1, Col3a1, and Postn. $n = 4$. Data are presented as mean ± SD. The data were analyzed using one-way ANOVA corrected by the post hoc Turkey's test

of the mTORC1 signaling pathway in vivo. Figure S5 showed that fibroblast-specific deletion of TRIM35 in TAC-induced mouse hearts led to decreased ubiquitination and protein level of SLC7A5 in isolated fibroblasts. However, these effects were reversed upon overexpression of SLC7A5 in fibroblasts isolated from Trim35^{cKO} mice (Figure S5). What is noteworthy is that while TRIM35 can catalyze the ubiquitination of SLC7A5, it may not be the sole E3 ligase responsible for this process in vivo, and other molecules may compensatively influence the ubiquitination modification of SLC7A5 and its protein stability when TRIM35 is deficient, as evidenced by obvious ubiquitination modification of SLC7A5 was detected in the fibroblasts isolated from SLC7A5-overexpressed-Trim35^{cKO} mouse hearts. Western blot analysis revealed that the TAC-induced increase in p-S6K and p-4E-BP1 levels was significantly inhibited in the heart tissues of Trim35^{cKO} mice, but reversed after overexpressing SLC7A5 (Fig. 9J-L). These findings suggest that TRIM35 induces cardiac remodeling at least

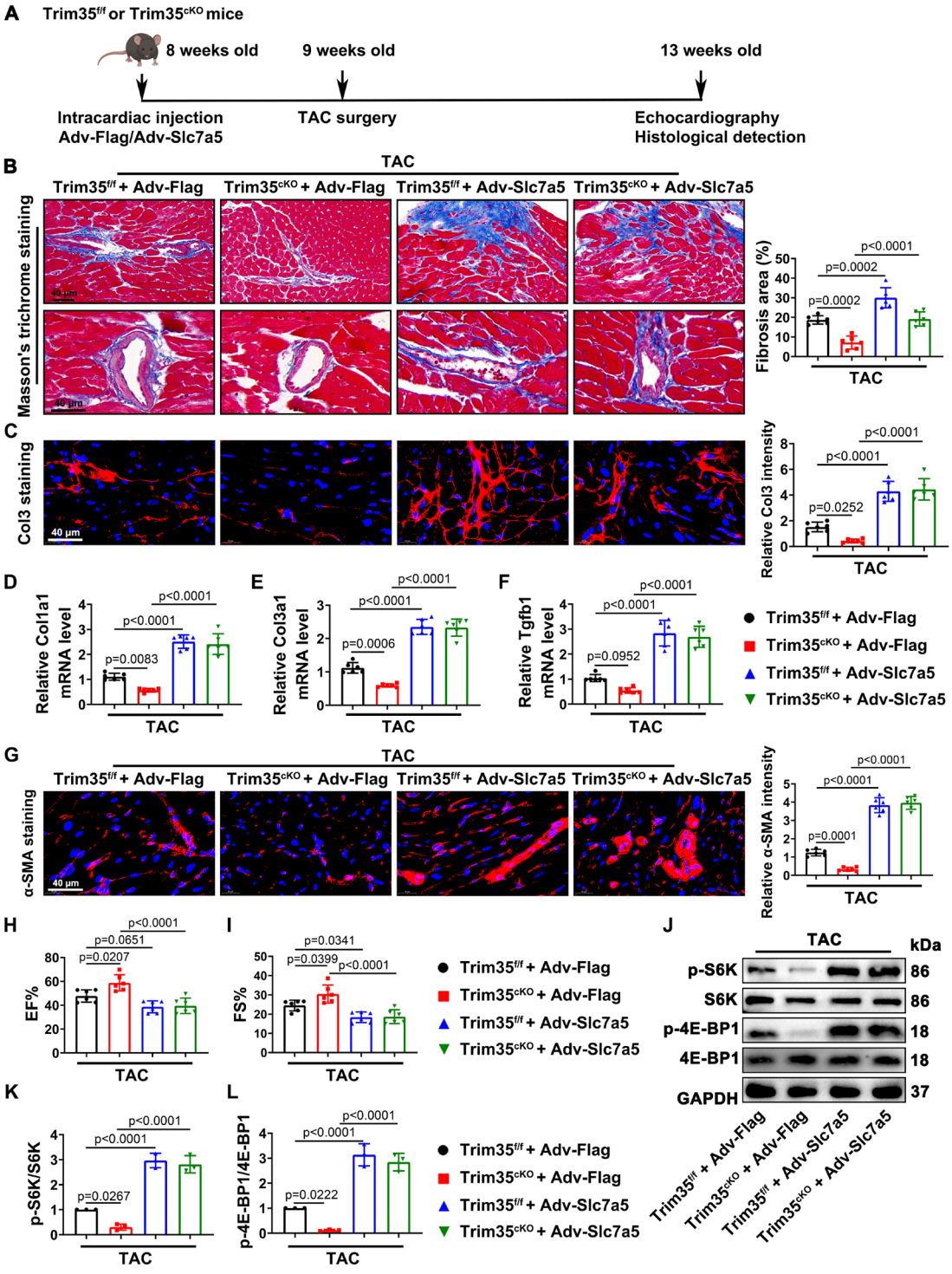

Fig. 9 The regulatory role of TRIM35 in cardiac fibrosis depends on SLC7A5. 8-week-old Trim35$^{f/f}$ or Trim35^{cKO} mouse hearts were transfected with Adv-Slc7a5 or Adv-Flag via intracardiac injection for one week before being subjected to TAC surgery for 4 weeks. **A** Treatment regimen. **B** Masson's trichrome staining was performed to detect myocardial interstitial and perivascular collagen deposition, and the statistical result of fibrosis was shown. $n = 6$. **C** Collagen deposition was analyzed by immunofluorescence staining with anti-Col3 antibody (red), and the statistical result of relative Col3 intensity was shown. $n = 6$. **D-F** The mRNA levels of Col 1a1, Col 3a1, and Tgfb1. All normalized to HPRT. $n = 6$. **G** Fibroblast differentiation was analyzed by immunofluorescence staining with anti-α-SMA antibody (red), and the statistical result of relative α-SMA intensity was shown. $n = 6$. **H**, **I** Quantification of echocardiographic parameters of EF% and FS%. $N = 6$. **J-L** Representative Western blots and statistical results of p-S6K and p-4E-BP1 in mouse hearts. $n = 3$. Data are presented as mean ± SD. The data were analyzed using one-way ANOVA corrected by the post hoc Turkey's test

partially by up-regulating SLC7A5 via ubiquitination modification in fibroblasts.

TRIM35 triggers cardiac hypertrophy via SLC7A5

Next, we sought to verify whether TRIM35 regulates cardiac hypertrophy through SLC7A5. TAC-mice with a fibroblast-specific deficiency of TRIM35 exhibited a smaller heart size and a lower HW/BW ratio. However, when SLC7A5 was overexpressed, these mice showed an increased heart size and a higher HW/BW ratio (Figs. 10A and 11, B). Echocardiographic analysis revealed a dramatic decrease in IVS and LVPW in TAC-Trim35^{cKO} mouse hearts, but these parameters were significantly increased when SLC7A5 was overexpressed (Fig. 10C-F). H&E staining showed a reduction in the cross-sectional area of cardiac myocytes in the TAC-induced TRIM35^{cKO} mice, which was markedly reversed by overexpression of SLC7A5 (Fig. 10G). qRT-PCR analysis revealed that TRIM35-specific deficiency in fibroblasts suppressed the mRNA expression of hypertrophy-related genes ANP, BNP, and β-MHC, while overexpression of SLC7A5 significantly elevated the mRNA levels of these genes (Fig. 10H-J). These findings suggested that TRIM35 triggers cardiac hypertrophy at least partially by up-regulating SLC7A5.

Discussion

Ventricular remodeling entails structural and functional alterations in the ventricular chambers of the heart [1]. Dysregulation of cardiac fibroblasts leads to adverse

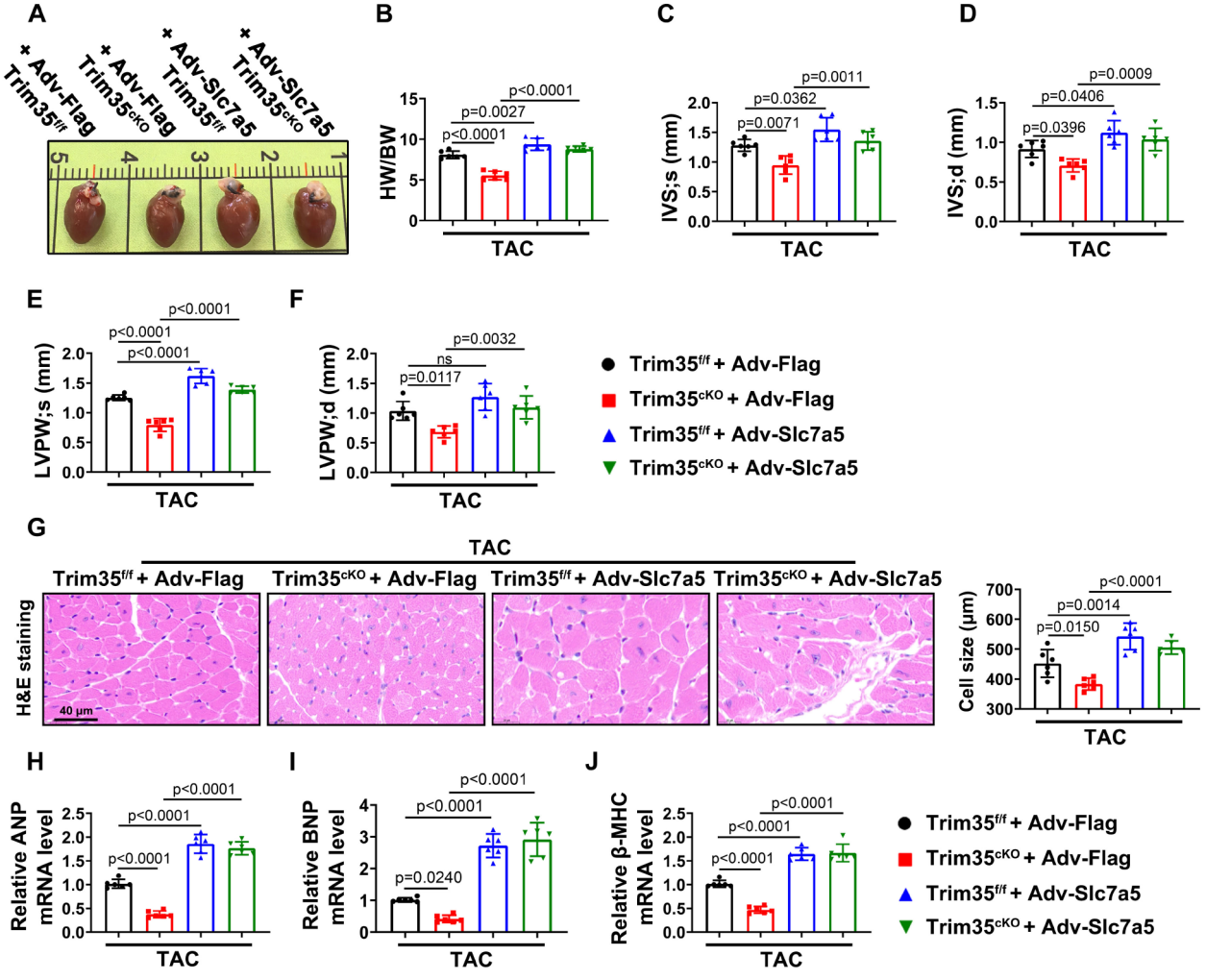

Fig. 10 The regulatory role of TRIM35 in cardiac hypertrophy depends on SLC7A5. 8-week-old Trim35$^{f/f}$ or Trim35^{cKO} mouse hearts were transfected with Adv-Slc7a5 or Adv-Flag via intracardiac injection for one week before being subjected to TAC surgery for 4 weeks. **A** Representative gross appearance of whole hearts. **B** The ratio of HW/BW. $n=6$. **C-F** Quantification of echocardiographic parameters includes IVS; s, IVS; d, LVPW; s, and LVPW; d. $n=6$. **G** H&E staining were performed to detect cardiomyocyte cross-sectional area, and the statistical result of cell size was shown. $n=6$. **H-J** The mRNA expression of ANP, BNP, and β-MHC were analyzed by qRT-PCR. $n=6$. Data are presented as mean ± SD. The data were analyzed using one-way ANOVA corrected by the post hoc Turkey's test

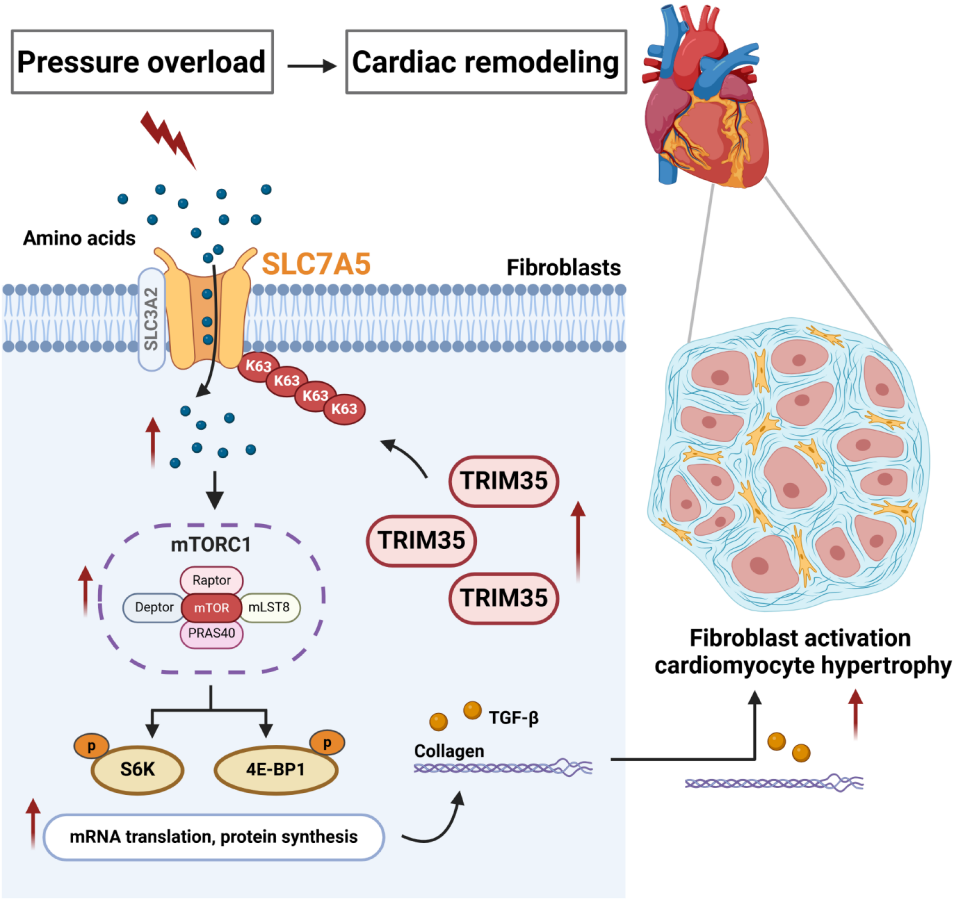

Fig. 11 Schematic depiction of the regulatory mechanism in which TRIM35 interacts with and catalyzes K63-linked ubiquitination of SLC7A5 to up-regulate its protein level in cardiac fibroblasts, thereby enhancing amino acid transport and mTORC1 activation during cardiac remodeling. TRIM35 promotes cardiomyocyte hypertrophic growth through paracrine signaling

ventricular remodeling, characterized by excessive collagen deposition, fibrosis, and alterations in cardiac function [4]. Understanding the molecular mechanisms underlying cardiac fibroblast function and ventricular remodeling is crucial for developing novel therapeutic strategies for preventing heart failure. This study provides evidence that TRIM35, which is abnormally expressed in fibroblasts in both murine and human fibrotic hearts, plays a pivotal role as a pro-fibrotic factor, amplifying cardiomyocyte hypertrophic growth through paracrine signaling. Through a comprehensive mechanistic exploration, we have unveiled a novel pathway in which TRIM35 targets and up-regulates the amino acid transporter SLC7A5, facilitating amino acid transport and subsequent activation of mTORC1 signaling. By shedding light on the intricate interplay between fibroblast-TRIM35 and adverse ventricular remodeling, this research not only deepens our understanding of cardiac pathophysiology but also uncovers a previously unknown molecular regulatory mechanism governing amino acid transport in cardiac fibroblasts.

Although current researches have revealed the involvement of TRIM35 in tumor growth, viral infections [20], inflammatory responses [14], embryonic development [16], and kidney injury [19], the breadth and depth of research on TRIM35 are far less extensive compared to other proteins in the TRIM family, such as TRIM21, TRIM72, and TRIM25 [5]. Recently, seminal studies have reported that TRIM35 inhibits LSD1 demethylase activity through K63-linked ubiquitination and enhances anti-tumor immunity [14]. TRIM35 mediates protection against influenza infection by degrading viral PB2 [20]. TRIM35-mediated TIGAR ubiquitination degradation suppresses mitochondrial fusion and aggravates renal ischemia-reperfusion injury [19]. These pieces of evidence suggest that TRIM35-mediated processes involving critical protein turnover and stability may play a key role in the development of multiple diseases. It is noteworthy that a recent study suggests that TRIM35-mediated degradation of nuclear PKM2 destabilizes GATA4/6 and induces P53 in cardiomyocytes, thereby promoting heart failure [17]. Their study highlights the significant role of TRIM35 in cardiomyocyte function and the

progression of heart failure [17]. Ventricular adverse remodeling is also a crucial factor during the development of heart failure. Our study reveals that TRIM35 is up-regulated in fibroblasts in murine and human hearts and is associated with the progression of cardiac fibrosis. The previous study lacked mechanistic insight into the signaling pathways resulting in TRIM35 induction, and we found that the expression of TRIM35 responds to TGF-β1 stimulation in NRCFs, indicating that inhibiting the TGF-β1 dependent signal may be an effective strategy to suppress TRIM35 expression. It also has not been studied whether TRIM35 inhibition can protect against the progression of heart failure. Here, we reported that conditional knockout of TRIM35 in fibroblasts inhibits the progression of myocardial fibrosis and suppresses cardiomyocyte hypertrophic growth through paracrine signaling. Our findings firstly underscore the significant role of TRIM35 in myocardial fibrosis. Additionally, we reveal that TRIM35 deficiency in fibroblasts may represent a key strategy for preventing the onset and progression of heart failure.

Transporters are membrane proteins that facilitate the selective transfer of organic and inorganic solutes across the plasma membrane and membranes of intracellular organelles [34]. They play a crucial role in cellular uptake and epithelial absorption of essential nutrients, including sugars, amino acids, lipids, vitamins, and minerals [35]. The TRIM family plays a crucial role in regulating membrane repair through various mechanisms such as ubiquitination, protein-protein interactions, and modulation of signaling pathways [5]. They also exert influence on membrane proteins in cells [21]. For example, TRIM21 inhibits the replication of various IAV subtypes by targeting matrix protein 1 (M1), the most abundant structural protein located inside the envelope membrane in virions [36]. Here, we reported the molecular mechanism by which TRIM35 regulates the membrane channel protein SLC7A5. Solute carrier (SLC) family transporters facilitate the transportation of a wide range of molecules, encompassing neurotransmitters, fatty acids, amino acids, and inorganic ions [37]. SLC7A5 belongs to the SLC family of transporters and is responsible for transporting essential amino acids [28]. It was reported that deletion of Slc7a5 gene in neurons affects the postnatal metabolic state, resulting in a shift in lipid metabolism [23]. Mutation of SLC7A5 supports an essential role for branched-chain amino acids (BCAAs) in human brain function [38]. This study found that TAC surgery significantly up-regulates SLC7A5, which is among the top 50 up-regulated genes in fibrotic cardiac tissues. Knockdown of Slc7a5 in myofibroblasts significantly inhibits pressure overload-induced cardiac fibrosis, suggesting that SLC7A5 play a crucial role in the underlying mechanisms of cardiac fibrosis. Additionally, the present study found no correlation between the gene levels of Trim35 and Slc7a5 in patient hearts with HCM. In this study, we demonstrated that TRIM35 can up-regulate the protein level of SLC7A5 involving K63-linked ubiquitination. However, we observed that TRIM35^{cKO}-Sham-mice did not show a down-regulation of SLC7A5, p-S6K, and p-4E-BP1 protein levels (Figs. 6E and 7C), indicating that this regulatory mechanism may be stress-dependent under pressure overload. Here, we discovered that TRIM35 affects the abundance of SLC7A5 in cardiac fibroblasts through a post-translational modification pathway.

Recent advances, particularly in the field of cardiac fibrosis, have highlighted the role that metabolic reprogramming plays in the pathogenic phenotype of myofibroblasts [39]. Amino acids, such as leucine, glutamine, and arginine, serve as indispensable components for supporting collagen matrix production and promote cell growth by activating mTORC1 in cardiac fibroblasts [24, 28]. Activation of mTORC1 has been associated with promoting fibroblast proliferation, migration, and extracellular matrix synthesis, thereby contributing to tissue repair and fibrotic processes [40]. It has been reported leucine and arginine, can stimulate mTORC1 activity independently of growth factors [41]. Amino acid availability leads to the recruitment of mTORC1 to the lysosomal membrane through the Rag GTPases [42]. Subsequently, mTORC1 phosphorylates downstream targets such as S6K1 and 4E-BP1, thereby promoting protein synthesis and cell growth [42]. Our in vitro experiments confirmed that TRIM35 mediates the up-regulation of SLC7A5 protein level, acting as a crucial upstream signal for amino acid transport. This, in turn, up-regulates the phosphorylation levels of S6K and 4E-BP1 in cardiac fibroblasts. For the first time, we have demonstrated that TRIM35 can regulate cellular amino acid transport through SLC7A5, suggesting that E3 activity-mediated ubiquitination modification is a pivotal mechanism in the regulation of amino acid transport.

The study also has limitations. Although our data show that sporadic expression of TRIM35 was observed in fibroblasts from non-remodeling human heart samples, these samples, obtained from patients with double-pore type atrial septal defects, are not ideal control specimens for comparison with the remodeling left ventricle. Therefore, the finding of abnormal up-regulation of TRIM35 in fibrotic human cardiac fibroblasts necessitates obtaining more comparable samples for further confirmation. This study has shown that fibroblast-specific knockout of the TRIM35 gene alleviates pressure overload-induced cardiac fibrosis, but it remains to be investigated whether targeting fibroblasts to overexpress TRIM35 will further exacerbate fibrosis or accelerate the progression of heart failure through mTORC1 signaling pathway. We

employed a cardiac adenoviral gene transfer approach to establish an animal model with SLC7A5 overexpression in the heart for investigating whether the regulatory function of TRIM35 on pressure overload-induced cardiac fibrosis depends on SLC7A5. Adv-Slc7a5 under the control of mouse cytomegalovirus (CMV) promoter is not specific to fibroblast. Therefore, developing a fibroblast-specific SLC7A5 expression mouse model is essential for advancing studies on cardiac fibrosis.

Conclusions

In summary, our findings demonstrate a novel role of fibroblast-TRIM35 in cardiac remodeling and uncover the mechanism underlying SLC7A5-mediated amino acid transport and mTORC1 activation. These results provide a potential therapeutic strategy for treating cardiac remodeling.

Abbreviations

TRIM35	Tripartite motif containing 35
TAC	Transverse aortic constriction
ECM	Extracellular matrix
mTORC1	Mammalian target of rapamycin complex 1
HCM	Hypertrophic cardiomyopathy
NRCFs	Neonatal rat cardiac fibroblasts
NRCMs	Neonatal rat cardiac myocytes
IVS	Interventricular septum thickness
LVPW	Left ventricular posterior wall thickness
ANP	Atrial natriuretic peptide
BNP	Brain natriuretic peptide
β-MHC	β-myosin heavy chain

Supplementary Information

The online version contains supplementary material available at https://doi.org/10.1186/s12964-024-01826-0.

Supplementary Material 1

Supplementary Material 2

Supplementary Material 3

Supplementary Material 4

Supplementary Material 5

Supplementary Material 6

Acknowledgements

Thanks to all the authors and funders who contributed to the article.

Author contributions

X.L., J.S., and X.J. were involved in the conceptualization of the study. X.L., J.S., and X.J. designed and implemented the methodology. X.L., B.S.Y., Z.X.W., K.F.N., and T.X.L. contributed to the investigations. X.L., J.S., X.J., T.T.T., S.J.L., L.H.S, Y.W., and C.X.S. performed the visualization of the data. X.L., X.J., S.J.L., and L.H.S. acquired funding for the studies. X.L., J.S., and X.J. administered the project. T.T.T., S.J.L., H.L., Y.W., and C.X.S. provided supervision for the study. X.L., J.S., X.J., B.S.Y., Z.X.W., K.F.N., T.X.L., T.T.T., S.J.L., L.H.S., Y.W., and C.X.S. were involved in the review and editing of the manuscript.

Funding

This work was supported by grants from the National Natural Science Foundation of China (No. 82300284, 82271592), Basic Research Foundation of Shanghai Sixth People's Hospital (No. ynqn202315) and Natural Science Foundation of Xiamen (No. 3502Z202373113, 3502Z202373112).

Data availability

No datasets were generated or analysed during the current study.

Declarations

Ethics approval and consent to participate

All animal protocols were performed in accordance with the Basel Declaration and the approval of the Animal Ethics Committee of Xiamen University (Approval No: XMULAC20220147; approved on 24 October 2022). An informed consent form was signed by all patients in accordance with the Declaration of Helsinki, and the study was approved by the Ethics Committee of Xiamen Cardiovascular Hospital (Approval No: KY2024-020-01; approved on 9 April 2024).

Consent for publication

Not applicable.

Competing interests

The authors declare no competing interests.

Author details

[1]Department of Cardiology, Shanghai Sixth People's Hospital Affiliated to Shanghai Jiao Tong University School of Medicine, Shanghai 200233, China
[2]Xiamen Cardiovascular Hospital, Xiamen University, Xiamen 361004, China
[3]Key Laboratory of Targeted Intervention of Cardiovascular Disease, Collaborative Innovation Center for Cardiovascular Disease Translational Medicine, Nanjing, China

Received: 24 May 2024 / Accepted: 11 September 2024
Published online: 20 September 2024

References

1. Frangogiannis NG. Cardiac fibrosis. Cardiovasc Res. 2021;117:1450–88.
2. Nakamura M, Sadoshima J. Mechanisms of physiological and pathological cardiac hypertrophy. Nat Rev Cardiol. 2018;15:387–407.
3. Wang M, Han X, Yu T, Wang M, Luo W, Zou C, Li X, Li G, Wu G, Wang Y, Liang G. OTUD1 promotes pathological cardiac remodeling and heart failure by targeting STAT3 in cardiomyocytes. Theranostics. 2023;13:2263–80.
4. Czubryt MP, Hale TM. Cardiac fibrosis: pathobiology and therapeutic targets. Cell Signal. 2021;85:110066.
5. Hatakeyama S. TRIM family proteins: roles in Autophagy, immunity, and Carcinogenesis. Trends Biochem Sci. 2017;42:297–311.
6. Lu Z, Hao C, Qian H, Zhao Y, Bo X, Yao Y, Ma G, Chen L. Tripartite motif 38 attenuates cardiac fibrosis after myocardial infarction by suppressing TAK1 activation via table 2/3 degradation. iScience. 2022;25:104780.
7. Chandler HL, Tan T, Yang C, Gemensky-Metzler AJ, Wehrman RF, Jiang Q, Peterson CMW, Geng B, Zhou X, Wang Q, et al. MG53 promotes corneal wound healing and mitigates fibrotic remodeling in rodents. Commun Biol. 2019;2:71.
8. Chen Y, Ding Y, Wang LM. Tripartite motif-containing 35 (TRIM35) is up-regulated in UUO-induced renal fibrosis animal model. Histol Histopathol. 2020;35:1427–35.
9. Chen L, Huang J, Ji YX, Mei F, Wang PX, Deng KQ, Jiang X, Ma G, Li H. Tripartite motif 8 contributes to pathological cardiac hypertrophy through enhancing transforming growth factor beta-activated kinase 1-Dependent Signaling pathways. Hypertension. 2017;69:249–58.
10. Liu J, Li W, Deng KQ, Tian S, Liu H, Shi H, Fang Q, Liu Z, Chen Z, Tian T, et al. The E3 ligase TRIM16 is a key suppressor of pathological cardiac hypertrophy. Circ Res. 2022;130:1586–600.
11. Shen Y, Zhang H, Ni Y, Wang X, Chen Y, Chen J, Wang Y, Lin J, Xu Y, Zhao JY, Cheng L. Tripartite motif 25 ameliorates doxorubicin-induced cardiotoxicity by degrading p85alpha. Cell Death Dis. 2022;13:643.
12. Borlepawar A, Rangrez AY, Bernt A, Christen L, Sossalla S, Frank D, Frey N. TRIM24 protein promotes and TRIM32 protein inhibits cardiomyocyte

hypertrophy via regulation of dysbindin protein levels. J Biol Chem. 2017;292:10180–96.
13. Ishiwata-Endo H, Kato J, Tonouchi A, Chung YW, Sun J, Stevens LA, Zhu J, Aponte AM, Springer DA, San H et al. Role of a TRIM72 ADP-ribosylation cycle in myocardial injury and membrane repair. JCI Insight. 2018; 3(22):e97898.
14. Tang F, Lu C, He X, Lin W, Xie B, Gao X, Peng Y, Yang D, Sun L, Weng L. E3 ligase Trim35 inhibits LSD1 demethylase activity through K63-linked ubiquitination and enhances anti-tumor immunity in NSCLC. Cell Rep. 2023;42:113477.
15. Chen Z, Wang Z, Guo W, Zhang Z, Zhao F, Zhao Y, Jia D, Ding J, Wang H, Yao M, He X. TRIM35 interacts with pyruvate kinase isoform M2 to suppress the Warburg effect and tumorigenicity in hepatocellular carcinoma. Oncogene. 2015;34:3946–56.
16. Yu T, Kuang H, Chen J, Lin X, Wu Y, Chen K, Zhang M, Zhang W, Wen Z. Tripartite-motif family protein 35 – 28 regulates microglia development by preventing necrotic death of microglial precursors in zebrafish. J Biol Chem. 2020;295:8846–56.
17. Lorenzana-Carrillo MA, Gopal K, Byrne NJ, Tejay S, Saleme B, Das SK, Zhang Y, Haromy A, Eaton F, Mendiola Pla M, et al. TRIM35-mediated degradation of nuclear PKM2 destabilizes GATA4/6 and induces P53 in cardiomyocytes to promote heart failure. Sci Transl Med. 2022;14:eabm3565.
18. Fang Y, Lu ZH, Liu BZ, Li N, Yang MZ, Wang P. IRF5 promotes glycolysis in the progression of hepatocellular carcinoma and is regulated by TRIM35. J Dig Dis. 2023;24:480–90.
19. Du Y, Chu CM, Zhuo D, Ning JZ. The inhibition of TRIM35-mediated TIGAR ubiquitination enhances mitochondrial fusion and alleviates renal ischemia-reperfusion injury. Int J Biol Macromol. 2022;209:725–36.
20. Sun N, Jiang L, Ye M, Wang Y, Wang G, Wan X, Zhao Y, Wen X, Liang L, Ma S, et al. TRIM35 mediates protection against influenza infection by activating TRAF3 and degrading viral PB2. Protein Cell. 2020;11:894–914.
21. Wang Y, Yan S, Yang B, Wang Y, Zhou H, Lian Q, Sun B. TRIM35 negatively regulates TLR7- and TLR9-mediated type I interferon production by targeting IRF7. FEBS Lett. 2015;589:1322–30.
22. Wei Y, Geng S, Si Y, Yang Y, Chen Q, Huang S, Chen X, Xu W, Liu Y, Jiang J. The Interaction between Collagen 1 and high mannose type CD133 Up-Regulates glutamine transporter SLC1A5 to promote the tumorigenesis of Glioblastoma Stem cells. Adv Sci (Weinh). 2024;11:e2306715.
23. Knaus LS, Basilico B, Malzl D, Gerykova Bujalkova M, Smogavec M, Schwarz LA, Gorkiewicz S, Amberg N, Pauler FM, Knittl-Frank C, et al. Large neutral amino acid levels tune perinatal neuronal excitability and survival. Cell. 2023;186:1950–67. e1925.
24. Meng Q, Xie Y, Sun K, He L, Wu H, Zhang Q, Liang T. ALYREF-JunD-SLC7A5 axis promotes pancreatic ductal adenocarcinoma progression through epitranscriptome-metabolism reprogramming and immune evasion. Cell Death Discov. 2024;10:97.
25. Lu Y, Hao C, Yu S, Ma Z, Fu X, Qin M, Ding M, Xu Z, Fan L. Cationic amino acid transporter-1 (CAT-1) promotes fibroblast-like synoviocyte proliferation and cytokine secretion by taking up L-arginine in rheumatoid arthritis. Arthritis Res Ther. 2022;24:234.
26. Bertero T, Oldham WM, Grasset EM, Bourget I, Boulter E, Pisano S, Hofman P, Bellvert F, Meneguzzi G, Bulavin DV, et al. Tumor-stroma mechanics coordinate amino acid availability to sustain Tumor Growth and Malignancy. Cell Metab. 2019;29:124–e140110.
27. Brisson BK, Stewart DC, Burgwin C, Chenoweth D, Wells RG, Adams SL, Volk SW. Cysteine-rich domain of type III collagen N-propeptide inhibits fibroblast activation by attenuating TGFbeta signaling. Matrix Biol. 2022;109:19–33.
28. Xu J, Jiang C, Cai Y, Guo Y, Wang X, Zhang J, Xu J, Xu K, Zhu W, Wang S, et al. Intervening upregulated SLC7A5 could mitigate inflammatory mediator by mTOR-P70S6K signal in rheumatoid arthritis synoviocytes. Arthritis Res Ther. 2020;22:200.
29. Onishi Y, Hiraiwa M, Kamada H, Iezaki T, Yamada T, Kaneda K, Hinoi E. Hypoxia affects Slc7a5 expression through HIF-2alpha in differentiated neuronal cells. FEBS Open Bio. 2019;9:241–7.
30. Zheng T, Chen W, Wang X, Cai W, Wu F, Lin C. Circular RNA circ-FAM158A promotes retinoblastoma progression by regulating miR-138-5p/SLC7A5 axis. Exp Eye Res. 2021;211:108650.
31. Lu X, He Y, Tang C, Wang X, Que L, Zhu G, Liu L, Ha T, Chen Q, Li C, et al. Triad3A attenuates pathological cardiac hypertrophy involving the augmentation of ubiquitination-mediated degradation of TLR4 and TLR9. Basic Res Cardiol. 2020;115:19.
32. Song J, Zhu Y, Li J, Liu J, Gao Y, Ha T, Que L, Liu L, Zhu G, Chen Q, et al. Pellino1-mediated TGF-beta1 synthesis contributes to mechanical stress induced cardiac fibroblast activation. J Mol Cell Cardiol. 2015;79:145–56.
33. Lu X, Yang B, Qi R, Xie Q, Li T, Yang J, Tong T, Niu K, Li M, Pan W, et al. Targeting WWP1 ameliorates cardiac ischemic injury by suppressing KLF15-ubiquitination mediated myocardial inflammation. Theranostics. 2023;13:417–37.
34. Mendes Ribeiro AC, Brunini TM, Ellory JC, Mann GE. Abnormalities in L-arginine transport and nitric oxide biosynthesis in chronic renal and heart failure. Cardiovasc Res. 2001;49:697–712.
35. Zhang L, Yan F, Li L, Fu H, Song D, Wu D, Wang X. New focuses on roles of communications between endoplasmic reticulum and mitochondria in identification of biomarkers and targets. Clin Transl Med. 2021;11:e626.
36. Lin L, Wang X, Chen Z, Deng T, Yan Y, Dong W, Huang Y, Zhou J. TRIM21 restricts influenza a virus replication by ubiquitination-dependent degradation of M1. PLoS Pathog. 2023;19:e1011472.
37. Lin L, Yee SW, Kim RB, Giacomini KM. SLC transporters as therapeutic targets: emerging opportunities. Nat Rev Drug Discov. 2015;14:543–60.
38. Tarlungeanu DC, Deliu E, Dotter CP, Kara M, Janiesch PC, Scalise M, Galluccio M, Tesulov M, Morelli E, Sonmez FM, et al. Impaired amino acid transport at the blood brain barrier is a cause of Autism Spectrum Disorder. Cell. 2016;167:1481–e14941418.
39. Zhao X, Kwan JYY, Yip K, Liu PP, Liu FF. Targeting metabolic dysregulation for fibrosis therapy. Nat Rev Drug Discov. 2020;19:57–75.
40. Zhao QD, Viswanadhapalli S, Williams P, Shi Q, Tan C, Yi X, Bhandari B, Abboud HE. NADPH oxidase 4 induces cardiac fibrosis and hypertrophy through activating Akt/mTOR and NFkappaB signaling pathways. Circulation. 2015;131:643–55.
41. Wyant GA, Abu-Remaileh M, Wolfson RL, Chen WW, Freinkman E, Danai LV, Vander Heiden MG, Sabatini DM. mTORC1 activator SLC38A9 is required to Efflux essential amino acids from Lysosomes and use protein as a nutrient. Cell. 2017;171:642–e654612.
42. Zheng L, Zhang W, Zhou Y, Li F, Wei H, Peng J. Recent advances in understanding amino acid sensing mechanisms that regulate mTORC1. Int J Mol Sci. 2016; 17(10):1636.

Publisher's note